Developmental exposure to chlordecone induces transgenerational effects in somatic prostate tissue which are associated with epigenetic histone trimethylation changes

Louis Legoff, Shereen Cynthia D'cruz, Morgane Lebosq, Aurore Gely-Pernot, Katia Bouchekhchoukha, Christine Monfort, Pierre-Yves Kernanec, Sergei Tevosian, Luc Multigner, Fatima Smagulova

Environment International 152 (2021) 106472

Contents lists available at ScienceDirect

Environment International

journal homepage: www.elsevier.com/locate/envint

Developmental exposure to chlordecone induces transgenerational effects in somatic prostate tissue which are associated with epigenetic histone trimethylation changes

Louis Legoff [a,1], Shereen Cynthia D'Cruz [a,1], Morgane Lebosq [a], Aurore Gely-Pernot [a], Katia Bouchekhchoukha [a], Christine Monfort [a], Pierre-Yves Kernanec [a], Sergei Tevosian [b], Luc Multigner [a], Fatima Smagulova [a,*]

[a] Univ. Rennes, EHESP, Inserm, Irset (Institut de recherche en santé, environnement et travail) – UMR_S 1085, F-35000 Rennes, France
[b] University of Florida, Department of Physiological Sciences, Box 100144, 1333 Center Drive, 32610 Gainesville, FL, USA

ARTICLE INFO

Handling Editor: Hefa Cheng

Keywords:
Chlordecone
Prostate
PIN
Transgenerational inheritance
Epigenetics
DOHaD

ABSTRACT

Background: Chlordecone (CD), also known as Kepone, is an organochlorine insecticide that has been used in banana crops in the French West Indies. Due to long-term contamination of soils and water, the population is still exposed to CD. Exposure to CD in adulthood is associated with an increased risk of prostate cancer (PCa).
Objectives: We examined the transgenerational effects of CD on murine prostate tissue.
Methods: We exposed pregnant Swiss mice to CD. The prostates from directly exposed (F1) and non-exposed (F3) male progeny were analyzed. We used immunofluorescence, RNA-seq and ChIP-seq techniques for the comprehensive analyses of chromatin states in prostate.
Results: We observed an increased prostatic intraepithelial neoplasia phenotype (PIN) in both F1 and F3 generations. Transcriptomic analysis in CD-derived F1 and F3 prostate using RNA-seq revealed that 970 genes in F1 and 218 in F3 genes were differentially expressed. The differentially expressed genes in both datasets could be clustered accordingly to common biological processes, "cell differentiation", "developmental process", "regulating of signaling", suggesting that in both generations similar processes were perturbed. We detected that in both datasets several *Hox* genes were upregulated; in F1, the expression was detected mainly in *Hoxb* and *Hoxd,* and in F3, in *Hoxa* family genes. Using a larger number of biological replicates and RT-qPCR we showed that genes implicated in testosterone synthesis (*Akr1b3*, *Cyp11a1, Cyp17a1, Srd5a1*) were dramatically upregulated in PIN samples; *Cyp19a1,* converting testosterone to estradiol was elevated as well. We found a dramatic increase in *Esr2* expression both in F1 and F3 prostates containing PIN. The PIN-containing samples have a strong increase in expression of self-renewal-related genes (*Nanog, Tbx3, Sox2, Sox3, Rb1*). We observed changes in liver, F1 CD-exposed males have an increased expression of genes related to DNA repair, matrix collagen and inflammation related pathways in F1 but not in F3 adult CD-derived liver.
The changes in RNA transcription were associated with epigenetic changes. Specifically, we found a global increase in H3K4 trimethylation (H3K4me3) and a decrease in H3K27 trimethylation (H3K27me3) in prostate of F1 mice. ChIP-seq analysis showed that 129 regions in F1 and 240 in F3 acquired altered H3K4me3 occupancy in CD-derived prostate, including highest increase at several promoters of *Hoxa* family genes in both datasets. The alteration in H3K4me3 in both generations overlap 73 genes including genes involved in proliferation regulation, *Tbx2, Stat3, Stat5a, Pou2f3* and homeobox genes *Hoxa13, Hoxa9.*

* Corresponding author at: Irset-Inserm UMR 1085, 9 avenue du Prof. Léon Bernard, 35000 Rennes, France.
E-mail addresses: louis.legoff@inserm.fr (L. Legoff), shereen-cynthia.d-cruz-benard@inserm.fr (S.C. D'Cruz), morgane.lebosq@univ-rennes1.fr (M. Lebosq), aurore.gely-pernot@ehesp.fr (A. Gely-Pernot), katia.bouchekhchoukha@etudiant.univ-rennes1.fr (K. Bouchekhchoukha), christine.monfort@inserm.fr (C. Monfort), pierre-yves.kernanec@univ-rennes1.fr (P.-Y. Kernanec), stevosian@ufl.edu (S. Tevosian), luc.multigner@inserm.fr (L. Multigner), fatima.smagulova@inserm.fr (F. Smagulova).
[1] These authors equally contributed.

https://doi.org/10.1016/j.envint.2021.106472
Received 1 September 2020; Received in revised form 11 January 2021; Accepted 16 February 2021
Available online 10 March 2021

Conclusions: Our data suggest that developmental exposure to CD leads to epigenetic changes in prostate tissue. The PIN containing samples showed evidence of implication in hormonal pathway and self-renewal gene expression that have the capacity to promote neoplasia in CD-exposed mice.

1. Introduction

The role of epigenetics in the developmental origins of adult diseases is supported by growing scientific evidence from epidemiological and animal studies (Nathanielsz, 2006; Wadhwa et al., 2009). Gestational exposure to environmental factors is known to increase the risk for disease development later in life (Heindel and Vandenberg, 2015; Klukovich et al., 2019; Mamun et al., 2012). One of the keys to the augmented disease risk is associated with the errors in two rounds of dynamic epigenetic reprogramming that occurs in the pre- and post-implantation embryo (Reik et al., 2001). During the second reprogramming event, primordial germ cells are correctly reprogrammed to give rise to germ-cell lineage in both sexes (Reik et al., 2001). This event is accompanied by extensive DNA methylation changes as well as chromatin remodeling, wherein distinct histone marks are deposited to establish the epigenetic state at germ cells (Burton and Torres-Padilla, 2010; Morgan et al., 2005). However, the epigenetic state of a specific set of genes is protected from reprogramming and preserved throughout the developmental period in germ cells (Lesch et al., 2013). Therefore, any perturbations during this reprogramming period could have an impact on the fetus itself and their progeny because germ cells of an individual determine the germ and somatic cell fates of the subsequent generation (Lesch et al., 2013). However, during spermatogenesis, most of the histones are replaced by protamines, but up to 10% of histones are preserved in the sperm (Brykczynska et al., 2010). This histone-containing fraction is important for transmission of the paternal epigenetic information (reviewed in (Legoff et al., 2019b)). Recently, it was shown that a limited number of paternal sperm histones H3K4me3 is detected in the early embryo (Dahl et al., 2016; B. Zhang et al., 2016), supporting the fact that paternal histones can mediate transgenerational inheritance.

Several studies have contributed to our understanding of environmentally-induced transgenerational epigenetic inheritance through DNA methylation and histone modifications (Gely-Pernot et al., 2015; Hao et al., 2016; Niedzwiecki et al., 2012; Skinner et al., 2010). Studies conducted by us and others have shown that selected environmental toxicants such as DDT, atrazine, and chlordecone (CD) induce histone alterations that could be transmitted up to at least three generations (Ben Maamar et al., 2019; Gely-Pernot et al., 2018, 2015; Hao et al., 2016). For example, organochlorine insecticide CD, also known as Kepone, induces meiotic defects, reduces the spermatozoa numbers in F1 and F3 generations, and alters the genome-wide occupancy of histone H3K4me3 (trimethylation of lysine 4 at histone H3) mark in testis (Gely-Pernot et al., 2018). Most importantly, a limited number of H3K4me3 marks were conserved in both generations, which suggests the importance of certain regions in transmitting toxicant-promoted effects (Gely-Pernot et al., 2018). The transgenerational inheritance mechanisms appear to be conserved in bovine and humans based on sperm histone-containing fraction data, where 61% of the genes preserved their histones in sperm (Samans et al., 2014). Moreover, comparison of human (Samans et al., 2014) and mouse (B. Zhang et al., 2016) sperm histone datasets showed that 66% of genes that preserved their histones are also common, suggesting that sperm histone-containing fraction is conserved in these three species and mouse could be a model for human transgenerational studies. CD is not only a reproductive toxicant, but also a teratogenic and carcinogenic compound (Agency for Toxic Substances and Disease Registry, ATSDR, 2019). Experimental studies have shown that CD has well defined estrogen-like properties, both *in vitro* and *in vivo* (Eroschenko, 1981; Hammond et al., 1979), and is, therefore, a potent endocrine-disrupting chemical as well. Since CD was extensively used between 1973 and 1993 in the French West Indies and because it is resistant to environmental degradation (Cabidoche et al., 2009), populations including pregnant women are still exposed to CD (Guldner et al., 2010; Multigner et al., 2016). Epidemiological studies in the French West Indies have shown that (Boucher et al., 2013; Costet et al., 2015) men exposed to CD in postnatal life have an increased risk of prostate cancer (PCa) occurrence (Multigner et al., 2010). Since our experimental studies showed that animals are particularly susceptible to epigenetic alterations during development (Gely-Pernot et al., 2018; Legoff et al., 2019a), we sought to explore whether CD could increase the risk of pathologies as well as promote transgenerational inheritance in somatic tissue such as prostate. Since CD is primarily accumulated in liver, which is the the major detoxification organ and has the potential to affect many other organs, we decided to analyze the effects in liver as well.

Epigenetic mechanisms, including histone modifications, nucleosomal remodeling and chromosomal looping, contribute to the onset and progression of prostate cancer. Recent technical advances significantly increased our understanding of the genome-wide epigenetic regulation of gene expression in prostate cancer. Aberrant genomic distribution and global level of histone modifications, nucleosome repositioning at the gene promoter and enhancer regions, as well as androgen receptor-mediated chromosomal looping may lead to the silencing of tumor suppressor genes and the activation of proto-oncogenes. In addition, androgen receptor-induced chromosomal looping facilitates recurrent gene fusion in prostate cancer. Studies in epigenetic regulation have translational implications in the identification of new biomarkers and the development of new therapies in prostate cancer. The histone post-translational modifications are known to be involved in the development of prostate pathologies. The prominent histone methylation marks, H3K4me3 (transcriptional activation mark regulated by Trithorax-group of proteins) and H3K27me3 (repressive mark introduced by Polycomb Repressive Complex 2), play a crucial role in the onset and progression of PCa (reviewed in (Chen et al., 2010)). In addition to methylation, histone acetylation also plays a role in prostate disease (Fraga et al., 2005). Given the importance of histone modifications in PCa, it would be informative to analyze the involvement of these marks in the transgenerational inheritance of prostate pathologies and the role of sperm histones in mediating the effects because previous studies have shown the important role of sperm in transmitting several phenotypes transgenerationally (Lismer et al., 2020; Siklenka et al., 2015).

In this study, we show that exposure to CD during the crucial developmental window (embyonic days E6.5-E15.5) induces an increase in PIN phenotype, leads to changes in gene expression in prostate and liver and affects the H3K4me3 histone occupancy at developmental genes in both F1 and F3 generations.

2. Methods

2.1. Animal treatment

Outbred Swiss mice (RjOrl) were used for all experiments. After breeding, the day of the vaginal plug was considered E0.5. The CD exposure window was limited to a period between E6.5-E15.5, which corresponds to SGT, somatic-to-germline transition (Seisenberger et al., 2012). The CD (Santa Cruz, Dallas, Texas 75220, USA) dose used here (100 μg/ kg body weight/ day) is lower compared to the lowest-observed-adverse-effect level (LOAEL, 250 μg/ kg body weight/ day (ATSDR, 2019), a dose that does not cause any systemic toxicity. Biomonitoring surveys among French West Indies populations have shown

that internal exposure doses (chlordecone blood concentration) may reach 100 μg/l (Guldner et al., 2011). This corresponds to an external exposure dose of 20 μg/kg bw/d under steady state assumption (C. Emond, personal communication). Such external dose is sufficiently close to the dose used in our experimental study (100 μg/kb bw/d). Moreover, considering our observations that report an adverse effect at lower dose than the current LOAEL for mice (250 μg/kg bw/d), this may be considered by Health Regulatory Agencies to revise the current toxicological reference values that are used for public health management of chlordecone pollution in French West Indies.

In fact, at the start of the study, we tested three doses of CD in mice: 100, 250 and 1000 μg/ kg body weight/ day. Our preliminary results showed that 100 and 250 μg/ kg body weight/ day of CD induce similar effects, based on effect on spermatozoa count. Sperm counts were performed as previously described (Vallet-Erdtmann et al., 2004). To count the spermatozoa, briefly, epididymis was suspended in 1 ml of 0,05% Triton Triton-X100 buffer, incised and homogenized using a homogenizer (POLYTRON® PT 2500 E). One ml of 0,05% Triton-X100 buffer were added individually to the original homogenizing vessel and homogenized again. This process was repeated five times for each sample to obtain all spermatozoa in a final volume of 6 ml. Spermatozoa from each sample were then enumerated using a Malassez hemocytometer. Data were averaged and plotted in Excel, presented as total number of spermatozoa per epididymis compared to control. 1000 μg/ kg body weight/ day of CD was toxic and resulted in animal mortality. So, we opted to study the dose (100 μg/ kg body weight/ day) that is lower than the current LOAEL dose. CD is well absorbed and distributed throughout the body following exposure, and has a long half-life (Egle et al., 1978), and can pass the placental barrier (Huber, 1965). Also, it is likely to persist in the body for a long duration following exposure.

CD was suspended in olive oil and administered via oral gavage at a dose of 100 μg/ kg body weight/ day in a volume of 150 μl. The control mice were treated with the same volume of oil. For the CD group, male progeny of F0 females (ie. the pregnant mice administered with 100 μg/ kg body weight/ day of CD) were defined as F1 and were crossed with non-littermate untreated females to give rise to the F2 generation. Similarly, the male progeny of F2 was crossed with non-littermate untreated females to give rise to the F3 generation. The oil-derived control animals were processed and crossed in the same way as CD-treated group. We excluded F2 generation from all the experimental analyses as F2 mice are derived from F1 gametes that were embryonically exposed to CD. Since we were particularly interested in transgenerational inheritance of prostate pathologies, we analyzed the prostate of the completely non-exposed F3 generation. Anterior prostates from F1 and F3 generations were analyzed when the animals were approximately 6-month-old. For most of our experiments, we used a minimum of 4 biological replicates derived from independent, non-related treated mothers. The number of biological replicates used for each experiment, mentioned in the respective Methods sections, depends on the costs and experimental variability observed. The data from F1 CD-exposed mice (liver, prostate, sperm) were compared with the data from F1 oil-exposed control group counterparts; the data from F3 CD-derived group (liver, prostate) were compared with F3 oil-derived control counterparts.

2.2. Ethics approval

The animal facility used for the present study is licensed by the French Ministry of Agriculture (agreement D35–238–19). All animal procedures were performed according to the Ethics Committee of the Ministry of the Research of France (agreement number: 01861.02). All experimental procedures followed the ethical principles outlined in the Ministry of Research Guide for Care and Use of the Laboratory Animals and were approved by the local Animal Experimentation Ethics Committee (C2EA-07).

2.3. Prostate morphology analyses

To study prostate morphology, anterior prostate from F1 and F3 control mice and CD-treated groups were fixed in Bouin's solution for 24 h, washed in PBS and 70% ethanol, dehydrated and embedded in paraffin. 5 μm sections of the entire prostate were cut and sections were placed on glass slides. The sections were deparaffinized and stained with H&E. Pictures were taken with a digital slide scanner (NanoZoomer, HAMAMATSU) and analyzed using the NDPview software (v2.7.25). We used for the analysis, 40 animals from F1 (18 control, 22 CD) and 43 animals from F3 generations (19 control, 23 CD).

2.4. Immunofluorescence analysis of prostate tissue

For immunostaining, the prostates from F1 and F3 control and CD-treated groups were fixed at 4 °C in 4% (w/v) PFA solution containing PBS for 16 h, dehydrated and embedded in paraffin. The sections were cut with a microtome (Microm HM 355 S) at 5-μm thickness. The sections were deparaffinized and rehydrated, and the epitopes were unmasked in 0.01 M citrate buffer, pH 6 at 80 °C for 45 min. After washing in 1X PBS-0.05%Tween 20 (Sigma-Aldrich; PBS-T), the sections were incubated with rabbit anti-H3K4me3 (1:500, Abcam, Ab8580) or with mouse anti-H3K27me3 (1:200, Abcam, Ab6002) or rabbit polyclonal hyperacetylated histone 4 (1:500, Merck Millipore, 06-946) antibodies. The sections with primary antibodies were incubated in PBS-T overnight at 4 °C in a humidified chamber. After washing in PBS-T, the sections were incubated with an appropriate fluorescent secondary antibody (1:100; AlexaFluor from Invitrogen) for 1 h in a humidified chamber at room temperature. The sections were counterstained with Vectashield solution (Eurobio Scientific, France) containing 4,6-diamidino-2-phenylindole dihydrochloride (DAPI). The images were taken using an AxioImager microscope equipped with an AxioCam MRc5 camera and AxioVision software version 4.8.2 (Zeiss, Le Pecq, France) with a 5X or 40X objective lens using the same exposure time (DAPI, 350/442, Alexa Fluor 488, 488/525, Alexa Fluor 594, 594/617). The images were left unprocessed prior to analysis. We quantified fluorescence inside nuclei and analyzed a minimum of 250 cells per prostate, from at least 3 different sections using ImageJ software. At least 4 different prostates were used for each group. To consider the background, we drew manually a region of interest in a cell-free area for each picture. Residual background fluorescence could be generated by nonspecific binding of secondary antibodies; we observed that background is low compared to specific signal, but for accuracy the average intensity of background region was multiplied by the area of the cell and then subtracted from the total cell fluorescence.

2.5. RNA extraction, qPCR and RNA-seq

For the analysis of F1 and F3 prostates, total RNA was extracted by using the RNeasy plus mini kit (Qiagen, 74134) according to the manufacturer's instructions from the anterior prostates that were snap-frozen following dissections. The tissue was homogenized in a TissueLyser (Qiagen) using Tungsten carbide beads (Qiagen, 69997). The kit included a DNA elimination step using a column. The absence of DNA was confirmed by using RT reaction product without adding reverse transcriptase. The quality of RNA from all extracted tissue was always inspected by bioanalyzer before library preparation and absence of DNA was confirmed. For RT-qPCR analysis, minimum 5 biological replicates were used each from F1 and F3 control and CD-exposed mice. Reverse transcription was performed with 1 μg of RNA using the iScript Reverse Transcription kit (Invitrogen) according to the manufacturer's instructions. The resulting cDNA was diluted 10 times and used for quantitative PCR. qPCR was performed using Bio-Rad 384 plate machine using iTaq Universal SYBR Green Supermix (Biorad, 1725124). Ct values for *Rpl37*, a housekeeping gene, were used for normalization using CFX manager software provided with Biorad 384 plate machine. To select the

best housekeeping gene, we tested several common housekeeping genes such as *Rpl37a, Blm, Hprt, Actb* and found that *Rpl37a* expresses highly and does not show variations; the values are consistent between several experiments. The primer sequences used for qPCR are shown in Table S1. The genes for RT-qPCR analyses were selected based on RNA-seq data; plus some genes which are potentially implicated in PIN or altered in prostate cancer, including "stemness" genes, genes encoding alternative hormonal pathway factors and genes implicated in control of epigenetic regulation. The data were analyzed and are presented as mean values of Fold Change (FC) compared to control.

For the analysis of F1 and F3 liver, RNA from approximately 30 mg of liver was extracted using Trizol (Ambion, AM15596026) method. Tissue was placed in 1 ml of Trizol and disrupted with TissueLyser (Qiagen). Tungsten carbide beads (Qiagen, 69997) were used for sample disruption. After homogenization, the beads were removed, and the RNA extraction was performed according to the protocol provided by manufacturer. RNA concentration was quantified by Nanodrop. 5 μg of RNA was used for DNAse I treatment, using Turbo DNA-free kit (Ambion, AM1907) according to manufacturer's instructions. 1 μg RNA treated with DNAse I was used for reverse transcription. The cDNA synthesis, qPCR analysis and normalization were performed similar to prostate RT-qPCR analysis. For liver analysis, 8 biological replicates were used for F1 and F3 control and CD-derived groups.

For RNA-seq analysis, 3 biological replicates derived from unrelated males of F1 and F3 control or CD-derived prostate RNA were used to synthesize a strand-specific cDNA library. In F3, the CD-derived prostates were not selected based on their morphology which implies that the prostates could be PIN-positive or PIN-negative. RNA-seq analysis in F1 was performed in samples which were found to be PIN-positive. The libraries were prepared using the TrueSeq Stranded mRNA Sample Preparation kit (Diagenode), or stranded NEBNext® Ultra™ RNA Library Prep Kit for Illumina using minimum 1 μg of total RNA according to the protocol provided by the manufacturer. The sequencing of the libraries was processed on Illumina HiSeq4000 sequencer as paired-end 50 base reads. Image analysis and base calling were performed using RTA 2.7.3 and bcl2fastq 2.17.1.14. Adapter dimer reads were removed using DimerRemover. To analyze differentially expressed genes, first, the quality-checked reads were aligned to the reference genome [*Mus musculus* Ensembl mm10 sequence] using TopHat version 2.0.14 (–library-type = fr-firststrand, –mate-inner-dist = 100, –no-coverage-search) and Bowtie2 v2.1.0. Quantification of gene expression was performed using HTSeq v0.6.1 with an annotation file obtained from Ensembl (release 81). Read counts were normalized and compared between control and CD samples using DESeq2 v1.6.3. P-values were automatically adjusted for multiple testing by DESeq2 using the Benjamini and Hochberg method. The functional enrichment analysis of the Differentially Expressed Genes (DEGs) was performed using the web-based tools g:Profiler (Raudvere et al., 2019) with default parameters. Heatmap was generated with R package Pheatmap v1.0.12, using row clustering (Euclidian distance, or correlation method complete-linkage clustering) and scaling (scaling and centering).

2.6. Histone purification and Western blot (WB) analysis

Protein samples from F3 mouse prostate were prepared using the EpiSeeker Histone Extraction Kit (Abcam, 113476) according to the manufacturer's supplied protocol. Briefly, prostates were homogenized using TissueLyser (Qiagen) in Eppendorf tubes containing Tungsten carbide beads (Qiagen, 69997) and centrifuged at 900 g for 5 min. The pellets were resuspended in lysis buffer and left on ice for 30 min. After centrifugation, the supernatant fractions containing acid-soluble proteins were transferred to new tubes, and the Balance-DTT buffer was added. The protein concentrations were determined using the Pierce™ 660 nm Protein Assay (ThermoScientific, France). 5 μg of protein were run on a 4–15% Mini-Protean precast polyacrylamide gradient gel (BioRad, USA) for 1 h. Proteins were transferred onto ImmobilonPSQ membranes (Millipore, France) using an electro-blotter system (TE77X; Hoefer, USA) and modified Towbin buffer (48 mM Tris base, 40 mM glycine and 0.1% (wt/vol) SDS) and methanol (20% (vol/vol) anode; 5% (vol/vol) cathode) for 2 h. Subsequently, blocking was carried out using 5% skimmed milk in PBS-Tween 20 (0.05%) for 1 h. Proteins were detected using a rabbit polyclonal anti-trimethyl-Histone H3K4 (Millipore, 07-473; 1:10,000 dilution), or a rabbit polyclonal anti-histone H2A (Millipore, ABE327; 1:2000 dilution), or a mouse monoclonal anti-trimethyl-Histone H3K27 (Abcam, ab6002; 1:200 dilution), or a rabbit polyclonal anti-histone H3 (Abcam, ab1791; 1:1000 dilution), or a rabbit polyclonal anti-hyperacetylated histone 4 (Penta, Millipore, 06-946; 1:10,000 dilution), or a mouse monoclonal anti-H2B, clone 5HH2-2A8 (Millipore, 05-1352; 1:2000 dilution). The primary and the secondary antibodies were diluted in blocking solution (5% skimmed milk containing PBS-Tween 20 (0.05%)). The primary antibodies were detected using either rabbit (1:10,000 dilution) or mouse (1:5000 dilution) secondary antibodies conjugated to horseradish peroxidase (GE Healthcare, USA) for 1 h. The signals were developed using the ECL-Plus Chemiluminescence kit (GE Healthcare, USA) and the ImageQuant 350 system (GE Healthcare, USA). For band intensity analyses, ImageJ software was used to manually draw a rectangle over the first band. The same rectangle was dragged over to subsequent lanes vertically. Next, a plot peak profile (i.e. the relative density of the contents in the rectangle) for each lane was obtained. The plot peaks were closed to omit the background noise, and the closed plot peaks were selected to obtain the values corresponding to the band intensity area. The signal intensities of histone modifications were normalized against the band intensities from the corresponding unmodified H3 histone. The data are presented as normalized signal compared to control +/− SEM; we used 4 biological replicates for each group. The uncut original WB images are provided in supplementary Fig. S1.

2.7. Chromatin immunoprecipitation, ChIP-seq and ChIP-qPCR

ChIP from prostate tissue was performed as previously described (Gely-Pernot et al., 2015) with small modifications. Four anterior prostate lobes from different animals were pooled for each biological replicate. Tissue was fixed in 1% paraformaldehyde in PBS and quenched with 0.125 M Glycine. Tissue was homogenized in TissueLyser machine (Qiagen) using stainless steel beads (Qiagen, 69989) and pelleted. The pellet was lysed in 600 μl of Lysis buffer (1% SDS, 10 mM EDTA, 50 mM Tris-HCl pH 8) and sonication was performed by using Qsonica 700 sonicator supplied with cup horn 431C2 (Newtown, Connecticut, USA). Sonication was performed in 300 μl in Eppendorf tubes using the following conditions: efficiency 40%, sonication 10 sec on, 30 off, total time 6 min. Average size of the chromatin was 300 bp. We performed ChIP using 1 μg of H3K4me3 antibody (Merck Millipore, 07-473). Immunoprecipitated DNA was purified with the Qiagen MinElute kit. We performed the ChIP-seq experiment using two replicates of F1 or F3 prostate isolated from control or CD-exposed males. Sequencing libraries were prepared using the Diagenode MicroPlex Library Preparation kit (v2.02.15) at IGBMC, Strasbourg, France or performed by using NEBNext® ChIP-seq Library Prep Master Mix Set for Illumina® (NEB, E6240). The sequencing was processed on Illumina HiSeq4000 sequencer using a single-end 50-base read mode. Adapter dimer reads were removed using DimerRemover. The reads were mapped to the reference mm10 genome using Bowtie2 v2.2.7. The numbers of mapped reads were normalized by a scale factor to adjust the total number of reads. From the aligned reads, H3K4me3 peaks were identified using 2 biological replicates and the corresponding input by MACS2 (v2.1.1) algorithm; the following parameters were applied: a shift-size window of 73 bp, no model, and a p-value threshold $< 10e\text{-}05$. To compare the H3K4me3 ChIP datasets of the CD-treated and control samples, differential peaks were identified using the following steps: first, from all of the peaks called using MACS2, we retained only peaks with average values above the median; and second, we selected peaks with fold

changes above 1.5 or 2 and FDR < 0.05. Statistical significance was calculated using R package Limma v3.38.3 (Phipson et al., 2016), which was designed to work with a limited number of replicates. We performed functional annotation of the differential peaks using the web-based tool GREAT (McLean et al., 2010) v3.0.0 (default parameters). The differential peaks were visualized using the Integrative Genomics Viewer (IGV, v2.4.2).

For ChIP-qPCR, we used 5 control and 4CD-derived prostates. The primer sequences used for ChIP-qPCR are shown in Table S2. We chose for analysis, the regions which showed changes in F1, including the genes encoding the transcriptional factors, homeobox genes, transport, and metabolic genes. QPCR was carried out as described in the previous section. The internal region (far from promoter) of the *Gapdh* gene was used for background normalization. The data were analyzed and are presented as mean values of FC compared to control +/− SEM. The Wilcoxon-Mann-Whitney test was used to examine statistical significance. The summary of ChIP-seq and RNA-seq reads are provided in Table S3.

2.8. ChIP-qPCR in F1 and F3 sperm and protein extraction from sperm

This protocol was used for ChIP using H3 and H3K4me3 antibodies. The motile fraction of sperm was extracted from epididymis and ChIP was performed as described previously (Brykczynska et al., 2010). The ChIP was performed as described for prostate tissue but with small modifications. Spermatozoa from three mice for each biological replicate were fixed in 1% paraformaldehyde solution, quenched and pelleted. The pellet was lysed in 0.3 ml of SDS-DTT Lysis Buffer (1% SDS, 10 mM EDTA, 50 mM Tris-HCl pH 8, 10mMM DTT) containing 1X Protease Inhibitor Cocktail during 1 h at room temperature and sonicated with Qsonica sonicator using the following conditions: efficiency 60%, sonication 20 sec on, 2 off; total time 6 min. Average size of the chromatin was 300 bp. In total, 5 control and 4CD-exposed F1 sperm and for F3, we used 6 biological replicates for CD-derived and 6 for control group. QPCR was carried out as described in the previous section. Primers list is presented in Table S2.

For histone protein fraction, we centrifuged chromatin from ChIP experiment at 12000 rpm and 50 μl of supernatant was preserved for histone H3 analysis. To supernatant we added 2 μl of 5 M NaCl and performed reverse crosslink at 95 °C for 2 min. The concentration of reverse crosslinked proteins was measured, and 5 μg were analyzed by the WB. The H3 levels were normalized to major unspecific band detected in Red Ponceau stained membrane, which represent the total protein content. The data are presented as normalized H3 intensity compared to control +/− SEM.

2.9. Statistical analyses

We used the minimum number of animals according to the requirements of the EU ethic committee. The number of animals used was specified for each experimental procedure. To assess the statistical significance of PIN lesions in the prostate of mice, we performed Fisher's exact test which is more appropriate than Chi-squared when working with limited numbers (one of the expected frequencies in the contingency table was low (i.e., < 5)). As the number of biological replicates in each experiment was relatively low, we performed the non-parametric Wilcoxon-Mann-Whitney test to assess statistical significance in body weight measurements, qPCR experiments, immunofluorescence and Western blots quantifications. Difference in spermatozoa numbers counts were assessed by the non-parametric Kruskal-Wallis test and by pair-wise comparisons using the Wilcoxon-Mann-Whitney test. P-values were adjusted using the Benjamini and Hochberg method. For the statistical significance of RNA-seq data, Wald's test for generalized linear models implemented in R package DESeq2 was used. ChIP-seq data analysis was performed using the linear regression model method and the statistical significance was assessed by a moderated t-statistic, both implemented in the R package Limma. This R package, based on an Empirical Bayes method, was specifically designed to work with a limited number of replicates (Phipson et al., 2016). P-values of RNA-seq and ChIP-seq data were corrected for multiple testing by the Benjamini-Hochberg method, which is directly implemented in both R packages. Statistical significance for functional enrichment analysis were assessed using either binomial (GREAT), or hypergeometric (g:Profiler) tests, which were directly implemented in each of the tools used for the analyses.

3. Results

3.1. Morphological changes in the prostate of CD-derived F1 and F3 mice

To identify the effects of CD on prostate morphology, prostate sections stained using hematoxylin/ eosin (H&E) were used for histopathological analyses. Representative images from control and CD-exposed F1 mice at 20x and 40X magnifications are provided in Fig. 1. Sections from a minimum of 18 prostates for each group from F1 and F3 males were analyzed to identify the PIN phenotype. PIN lesions are characterized by increased epithelial cell proliferation with cells that form multilayers with enlarged dark nuclei and nucleoli. For each mouse, the prostate was classified as either PIN-positive or PIN-negative, and the data were presented as the incidence of PIN compared to the total number of evaluated prostates. The prostate sections from control mice showed normal tissue architecture with moderate to large acini lined with cuboidal to columnar epithelium and luminal infoldings. In contrast, the prostate sections from CD-exposed mice showed epithelial proliferation with a tufting pattern and nuclear enlargement that illustrates the typical features of PIN. In this study, the PIN phenotype was observed only in 5.5% (1 out of 18 prostates) in F1 and 5.3% (1 out of 19 prostates) in F3 control mice. In contrast, PIN phenotype was observed in 40.9% (9 out of 22 prostates) of the samples from CD-exposed F1 mice ($P = 0.0126$, Fisher exact test), and 30.4% (7 out of 23 prostates) of the samples from CD-derived F3 mice ($P = 0.0541$, Fisher exact test). These morphological changes in the prostate were accompanied by a 13% decrease in body weight of CD-exposed F1 mice compared to that of control (Fig. S2). In F3, we observed a similar tendency (9% decrease in the body weight of CD-derived mice) despite being not statistically significant (Wilcoxon-Mann-Whitney test, $W = 277.5$, $p = 0.066$) (Fig. S2). As previously shown (Gely-Pernot et al., 2018), exposure to 100 μg/kg bw/day of CD during development induced an almost 40% decrease in spermatozoa number in both CD-exposed F1 mice and CD-derived F3 mice (Fig. S3), exposure to 250 μg/kg bw/day of CD caused 50 and 32% decrease in spermatozoa number in both CD-exposed F1 mice and CD-derived F3 mice, respectively (Fig. S3).

3.2. RNA expression analyses revealed the increased expression of genes related to hormonal pathways, cellular proliferation, self-renewal and epigenetic regulation

We performed a genome-wide transcriptomic analysis by RNA-sequencing F1 PIN-containing prostates, and F3 without PIN selection due to limited number of PIN samples available at the start of the study when we conducted the F3 RNA sequencing. Our data showed that among the 22,491 transcripts identified in the prostate of F1 mice, 970 genes were differentially expressed (FC > 1.5, FDR < 0.1) in F1 and 218 in F3 (Table S4 & S5). The analysis of transcriptomics profiles revealed high heterogeneity within samples (Fig. S4, S5, S6). The variation could be explained by the outbred mouse strain background, which has somewhat high level of variability between samples and treatment may cause diverse response in exposed animals. To understand the molecular mechanisms associated with the phenotypic changes observed in both exposed F1 and the unexposed F3 generation, we performed functional annotation of differentially expressed genes (DEGs) using g:Profiler as described in the Methods. The functional annotation showed that

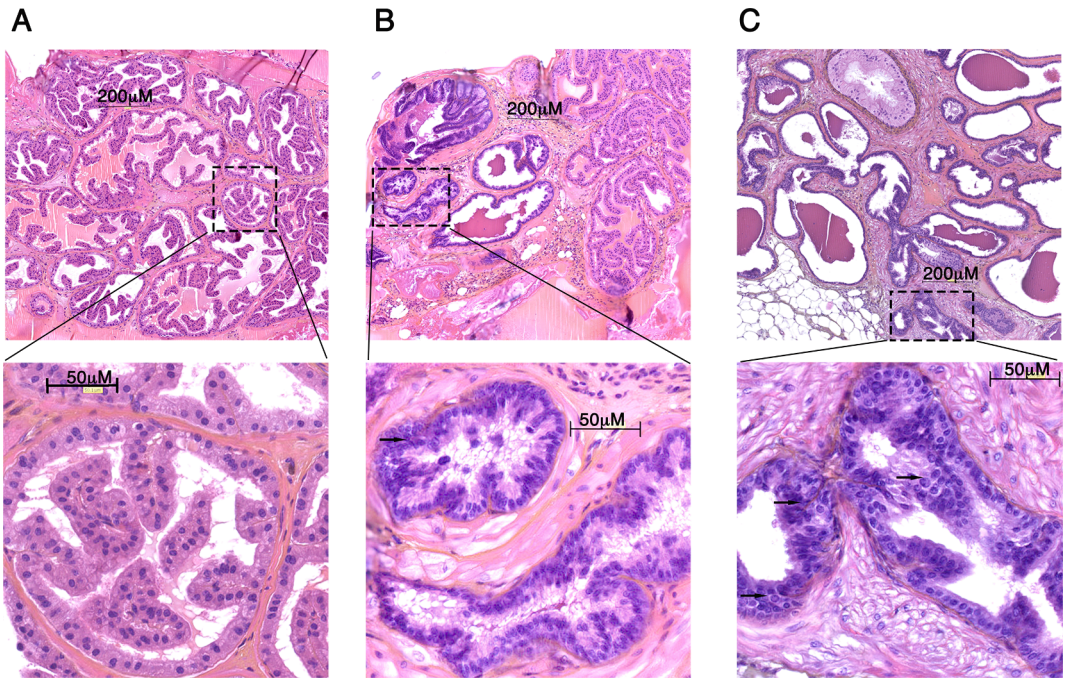

Fig. 1. Analysis of CD-exposed prostate tissue stained by hematoxylin and eosin (H&E) reveals the presence of PIN. Prostate sections of F1 control mice (A) and CD-exposed F1 mice (B, C) at 20X (upper panel) and 40X (lower panel) magnifications. In control tissue, cells with homogenous nuclei are observed (A); in CD-exposed the PIN phenotype is seen with epithelial proliferation, tufting pattern, nuclear enlargement and occasional crowds (indicated by arrows) that illustrates the typical features of PIN.

differentially expressed genes could be combined in several clusters in F1 and F3 datasets. Remarkably, in both F1 and F3, the significant clusters include common gene ontology terms "developmental process", "regulating of signaling", "cell differentiation", "regulation biological quality", suggesting that in both generations similar processes were perturbed (Fig. 2). Notably, the gene ontology term "developmental process" includes 18 homeobox genes including *Nkx3-1, Pou3f3, Tlx1, Emx2, Hoxb13, Hoxb3, Hoxb6, Hoxb7, Hoxb8, Hoxd3, Hoxd4, Hoxd8, Hoxd9,* in F1 and four genes in F3, *Hoxa3, Hoxa7, Hoxa9, Hoxa10*, suggesting strong impact of CD exposure on homeobox genes. We also detected steroid biosynthesis-related genes including *Apoe*, *Atp1a1*, *Ces1d*, *Cyb5r3*, *Cyp1a1*, *Ebp*, *Hrh1*, *Hsd3b7*, *Scarb1*, *Tecr* and *Wnt4* in F1 RNA-seq, suggesting possible impact of CD on steroidogenesis.

The common genes in two datasets include genes related to steroid hormone signaling (*Kiss1, Abhd2*), transcription *(Elf5, Foxp2, Zfp589*) and many genes encoding for the proteins of extracellular matrix region (*Isg15, Kiss1, Cpe, Fmod, Hebp2, Mme, Mt3, Olfm4, Optc, Kcnma1, Qsox1, Upk1a*), the complete set of DEGs are listed in Table S6.

The analysis of the samples with PIN by RT-qPCR, which include a larger number of biological replicates, helped to better understand the molecular network changes in the samples with PIN phenotype in both F1 and F3 generations. To this end, we analyzed the expression levels of genes involved in hormonal pathways, cellular proliferation, epigenetic regulation, stemness and the genes (Fig. 3A) that have been found to be deregulated in testis (Gely-Pernot et al., 2018).

Our RT-qPCR analysis showed that *Esr2* was dramatically over-expressed (18 times) in PIN-positive CD-exposed F1 prostates. Although these changes were less-dramatic in PIN-positive CD-derived F3 prostate, the expression of *Esr2* was still remarkably high (7-fold). Also, we observed that genes involved in cellular proliferation were strongly up-regulated in the prostate of CD-exposed mice (5-fold for *Asph* and 13-fold for *Ccnd1*). For *Asph,* the difference was less-pronounced in F3 compared to F1 with an observed fold-change of 2.7; while *Ccnd1* had 17.8-fold increase, the difference was not significant (Wilcoxon-Mann-Whitney, $W = 3$, $p = 0.056$). Notably, among the 8 genes involved in histone H3 trimethylation regulation, the lysine methyltransferase *Kmt2d* was up-regulated in F1 and F3 prostates. The most dramatic changes were observed in metabolic (*Fut4*) and signaling (*Tmc8*) related genes, that were over-expressed 167 and 473 times, respectively, and which are known to be deregulated in certain cancers, such as colon adenocarcinoma (Taniguchi et al., 2000) or hepatocellular carcinoma (Lu et al., 2017).

Since in resistant prostate cancers, an alternative pathway of hormonal biosynthesis was described, reviewed in (Armandari et al., 2014), we decided to assess the expression of steroidogenesis-related genes using RNA from PIN-containing samples. We found that *Akr1b3, Cyp11a1, Cyp17a1, Srd5a1* had dramatically increased expression; 2.3, 11.2, 11.4, 9.5 times respectively (Fig. 3A). The expression of *Cyp19a1,* a key enzyme converting testosterone to estradiol increased 3.4 times. The changes were significant in F1 but not in F3, suggesting that the direct effects of CD diminished with each generation.

In previous studies involving rodent models, it has been shown that early-life exposure to BPA reprograms prostate and enhances hormonal carcinogenesis (Prins et al., 2014). Thus, we asked whether prostates exposed to CD could have changes in their genes related to self-renewal. We found that expression of *Nanog* dramatically increased 31.3 times, the other tested genes, *Sox2, Sox3* and *Rb1,* had increased expression 7.5, 12.6, and 5.7 times, respectively in F1 mice (Fig. 3A). Our data reveals that CD exposure causes similar changes in "stemness" genes as observed in BPA study.

Next, we compared the altered regions found in our study with the gene expression data available from prostate cancer cell lines, to identify the human prostate cancer model closest to CD-derived prostate. Information on the gene expression of several prostate cancer cell lines including 33Rv1, DU145, LnCAP, PCA2b, NCI-H660 and PC-3 was obtained from the EMBL-EBI database. The basal gene expression was plotted as a heatmap, (Fig. 3B). Importantly, the genes which were highly differential in our PIN samples, such as *Esr1, Esr2, Cyp17a1, Cyp19a1, Pou2f3, Tfcp21l1* and *Sox2* had highest level of expression in NCI-H660 cell line. Besides that, some of *HOXA* genes (*HOXA1, HOXA4, HOXA9, HOXA10, HOTAIRM1, HOX-AS3, HOXA10-AS*) also have highest expression levels in the NCI-H660 cell line. This cell line is derived

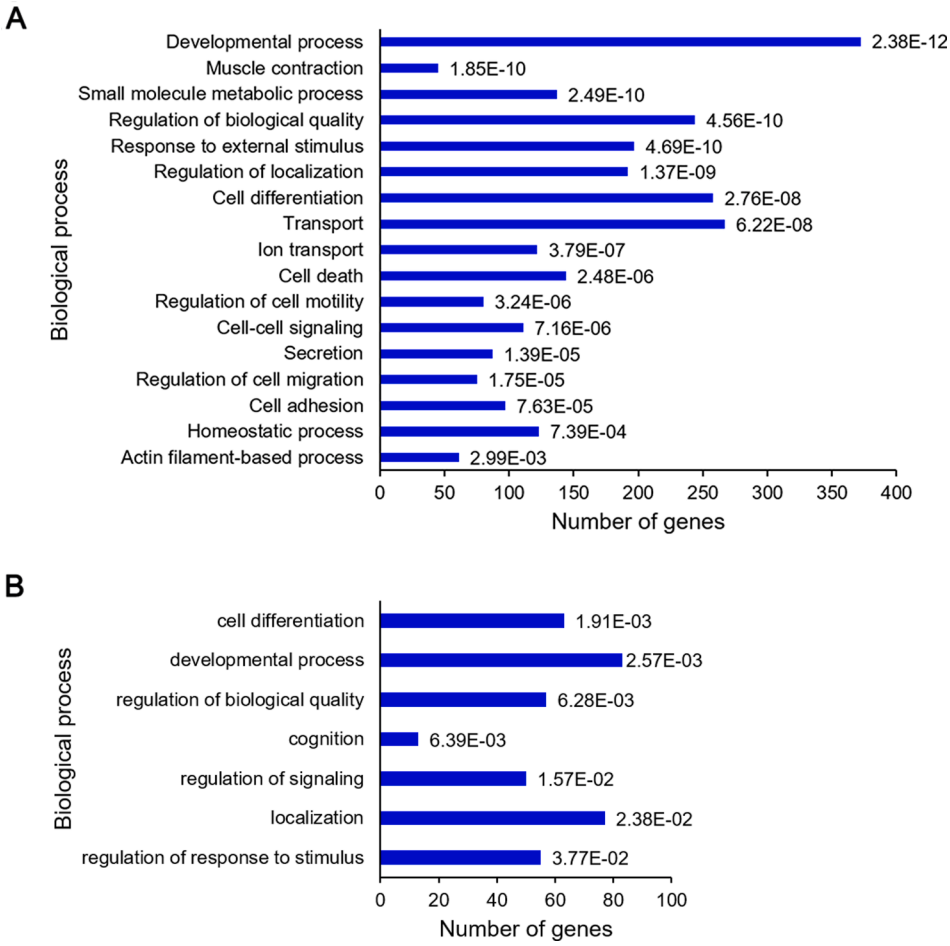

Fig. 2. Gene expression is affected by ancestral exposure to CD in the prostate of F1 and F3 mice. Functional annotation of differentially expressed genes in F1 (A) and in F3 (B). Clusters were identified by g:Profiler and gene ontology terms were sorted by adjusted p-value, the bars represent the number of genes per gene ontology terms.

from neuroendocrine prostate carcinoma, which is an aggressive variant of prostate cancer that may arise *de novo* in patients previously treated with hormonal therapies for prostate adenocarcinoma (Conteduca et al., 2019).

To sum up, our RNA expression analysis in PIN-containing samples showed a dramatic increase in the expression of genes related to hormonal biosynthesis, proliferation, self- renewal and extracellular matrix, and some of them were found to be highly expressed in neuroendocrine prostate adenocarcinoma.

3.3. Gestational exposure to CD leads to an up-regulation of genes involved in DNA repair, detoxification and inflammation in the liver

To address the effects of CD on detoxification of organs and assess the possible toxicity of the low dose that we used, we performed gene expression analysis in the liver of both F1 and F3 males. We performed RT-qPCR analysis of the genes involved in DNA repair, detoxification, regulation of lipid metabolic process and homeostatic-related functions as reported in previous studies using CD; it has been shown that exposure to CD induces liver injury (Tabet et al., 2016). Our analysis revealed that DNA repair genes are strongly up-regulated in the liver of CD-exposed F1 mice (Fig. S7 left). For example, single-strand break repair genes, *Ercc8* and *Parp1*, were over-expressed 4.0 and 8.9 times, respectively, in CD-exposed mice. We observed an increased expression of genes involved in double-strand break repair, such as *Atm* (7.9-fold), *Mre11a* (2.8-fold) and *Mus81* (2.3-fold). Genes involved in the regulation of lipid metabolic processes were also altered (3.6-fold for *Cyp17a1*, 2.4-fold for *Psap*). In addition, we also observed a significant increase in the expression of *Ccne2* (gene regulating cell cycle, 4.8 times), *Col1a2* (gene activated at liver fibrosis, 2.3-fold) and *Ifi27* (chemokine signaling pathway, 4.0-fold) in the liver of CD-exposed mice.

To determine whether these changes were maintained across generations, we evaluated their expression in the liver of CD-derived F3 mice. Our data revealed that most of the changes observed in F1 liver were restored in F3 to a normal level (Fig. S7 right). However, *Cyp17a1* was still up-regulated in the liver in F3 CD-derived mice compared to control mice (2.3-fold).

Our data suggest that direct exposure to CD leads to impairment in the expression of genes involved in DNA repair, cell cycle and lipid metabolism functions and that these changes are restored in the liver of F3 CD-derived mice.

3.4. Histone marks' occupancy is altered in the prostate of CD-derived F1 and F3 mice

Since changes in prostate morphology as well as RNA expression changes were observed in CD-derived F1 and F3 mice, we examined the epigenetic status of some of the important histone marks (H4ac, H3K27, H3K4) in the prostate. We immunostained tissue sections using antibodies against these marks and performed quantitative analysis of images using several biological replicates as described in the Methods section. Immunofluorescence analyses (IFA) revealed a global 50% decrease in the levels of H4ac and a 30% decrease in H3K27me3 signal in the prostate of CD-exposed F1 mice when compared to the control

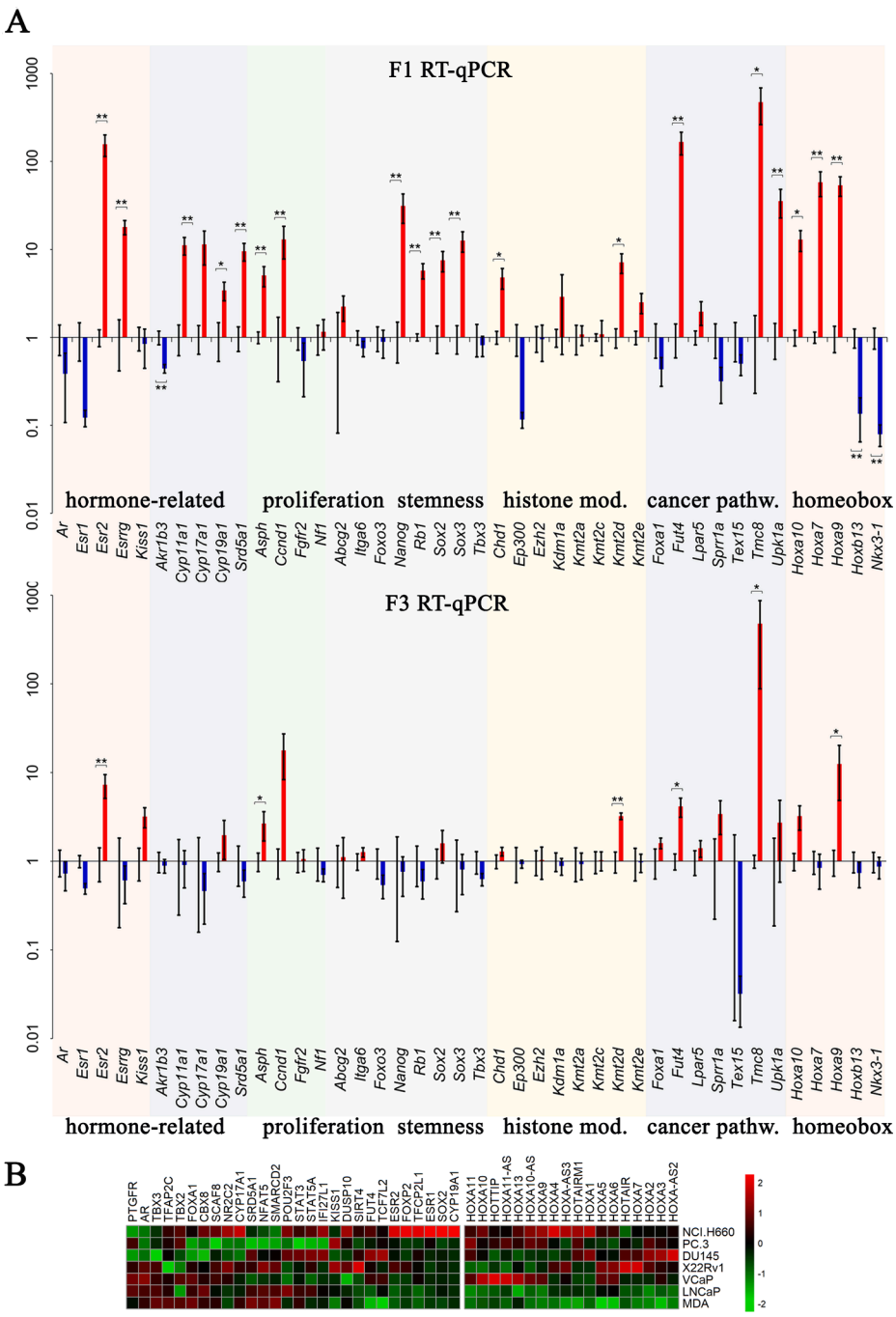

Fig 3. Gene expression in PIN phenotype prostate tissue in F1 and F3. (A) The analysis was performed by RT-qPCR. The upregulated genes are in red and downregulated in blue, *p < 0.05, **p < 0.01. (B) A heatmap showing the comparison of gene expression levels in human prostate cancer cell lines with important differentially expressed genes identified in our study. *HOXA* genes are presented as a separate heatmap. (For interpretation of the references to colour in this figure legend, the reader is referred to the web version of this article.)

(Fig. 4A&B). On the contrary, the levels of H3K4me3 tended to be increased 1.6 times in the prostate tissues (Fig. 4A&B) of the CD-exposed mice, while the p-value did not cross the significance threshold ($p = 0.057$). Analyses of the prostate tissues of CD-derived F3 mice showed that H3K4me3 levels were unchanged, while we observed a slight increase in the levels of H4ac (15%) and a decrease in H3K27me3 (15%) histone marks, although the changes were not statistically significant (Fig. S8). We analyzed the total levels of modified histones in purified histone fraction of the prostate of F3 generation mice by Western blot. We found that the levels of histone are not significantly changed in total protein fractions (Fig. S9). However, the protein levels tend to change in a similar way as immunofluorescence data.

3.5. A genome-wide H3K4me3 level shows increased occupancy in the prostate of CD-exposed F1 and F3 mice

Since H3K4me3 are important epigenetic histone marks associated with gene transcription and their levels were found to be increased in CD-exposed F1 prostate following immunofluorescence analyses, we sought to perform ChIP-seq of H3K4me3 to evaluate the genome-wide distribution of this mark in the prostate of CD-derived F1. We identified 775 regions, referred to as differential peaks, that displayed altered H3K4me3 occupancy in F1 CD-lineage prostate compared to control (FC > 1.5, FDR < 0.05) (Table S7 & Fig. S10). We identified genes located in the neighborhood of the most strongly altered peaks (FC > 2, 129 peaks) and performed a Gene Ontology (GO) enrichment analysis. Most of the differential peaks (92 out of 129) were found distally to the transcription start site (TSS) (<5kb), suggesting that they were not located at the

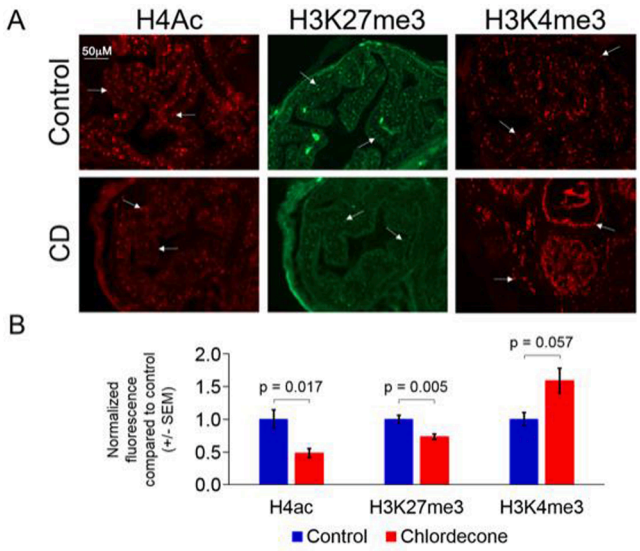

Fig. 4. The levels of H4ac and H3K27me marks were decreased and H3K4me3 is increased in the PIN-positive prostate of directly exposed F1 mice. (A) Representative images of prostate sections from control (Top panel) and CD-exposed (bottom panel) animals. Prostate cells were immunostained using anti-H4ac (red), anti-H3K27me3 (green) or anti-H3K4me (red) antibodies and images were taken and analyzed as described in the Methods section. White arrows show examples of the signals that we quantified. (B) Quantitative analysis of H4ac, H3K27me3 and H3K4me3 signals in nuclei was performed using ImageJ software and data are presented as relative fluorescence compared to control ± SEM. Values from control and exposed mice are displayed in blue and red, respectively. (For interpretation of the references to colour in this figure legend, the reader is referred to the web version of this article.)

promoter regions, but rather at enhancers. The GO enrichment analysis revealed that F1 differential peaks were situated in the vicinity of genes that are involved in prostate gland development (*Fgfr2*, *Foxa1*, *Hoxa13*, *Sox9*, *Stat5a*), tissue morphogenesis (*Etv2*, *Hoxa11*, *Jag2*, *Myc*, *Ncoa3*) and regulation of stem cell differentiation (*Tacstd2*, *Tbx5*, *Tgfbr3*, *Zfp36l2*) (Fig. 5A). Notably, we found that a 115 kb-long region of *Hoxa* genes (*Hoxa* cluster) displayed a global increase in H3K4me3 peak intensity in the prostate of CD-exposed mice (Fig. 5B) a detailed view of the region with the most highly increased H3K4me3 level (*Hoxa11/Hoxa11os*) is shown in Fig. S11.

Next, we aimed to determine whether F1 differential peaks could be detected in the F3 generation. To this end, we carried out H3K4me3 ChIP-seq in F3 prostate. We detected 240 differential peaks between control and CD-derived group Table S8. Of the differential peaks, 154 showed increased occupancy and 86 decreased occupancy, suggesting that H3K4me3 alteration in F3 is also in the similar direction. We compared F1 and F3 datasets and detected H3K4me3 changes in 73 common genes including genes which are known to be implicated in "positive regulation of proliferation" (*Pou2f3, Tbx2, Cbx8, Prl2c3, Ptgfr, Stat3, Stat5a*) and homeobox genes" (*Pou2f3, Hoxa9, Hoxa13*) among others (Fig. 5C). Full list of commonly altered genes is given in Table S9. For example, we detected altered H3K4Me3 in *Pou2f3* in F1 and F3 (Fig. 5D).

We confirmed our F3 ChIP-seq results with the F3 ChIP-qPCR by analyzing histone occupancy at the promoters of 22 regions. Out of these regions, 8 loci showed similar changes of in H3K4me3 mark in both generations (Fig. S12).

We found 83 common genes in F1 RNA-seq and ChIP-seq data (FC1,5, FDR0.1, FC2, FDR0.1, respectively), including important transcription factors (*Gata3, Nkx3-1, Pou2f3, Sox9, Tbx2, Tbx3, Ccnd1, Hoxb13, Hoxd11*). Full list is given on Table S10. In F3 RNA-seq and ChIP-seq data we detected 10 common genes with similar parameter of analysis, including homeobox *Hoxa9* and cell adhesion related gene, *Cdh12,* Table S11.

In summary, our results suggest that prenatal exposure to CD could lead to the altered epigenetic landscape in the vicinity of genes involved in prostate development and stem cell differentiation. Moreover, some of the changes are still detected in F3 generation suggesting that at least at some genes the epigenetic information was preserved.

3.6. ChIP-qPCR of H3K4me3 in CD-exposed F1 and F3 sperm shows decreased occupancy at Hoxa gene regions

To understand whether the epigenetic changes that we observed in prostate are preserved in sperm, we analyzed histone occupancy of H3K4me3 histone in the promoter of some genes using sperm from F1 and F3 mice. To this end, we performed the ChIP-qPCR analysis using sperm from control and exposed mice as described in the Methods section. The analysis showed a high ChIP-to-Input ratio in both F1 and F3 suggesting that the studied regions were preserved in sperm and avoided protamine replacement. We also observed the regions with no enrichment in sperm suggesting that H3K4me3 regions detected in prostrate are not preserved in sperm (e.g. *Ankib1, Mrgpra3, Tmod4*); alterations in these regions might occur due to other factors and not originated from sperm directly. In contrast to the prostate tissue, H3K4me3 occupancy in sperm has decreased in the vicinity of genes, including the homeobox genes *Hoxa3*, *Hoxa7*, *Kiss1* and *Nkx3-1* (Fig. 6A) in F1. The analysis in F3 males showed the changes in *Hoxa* genes, e.g. *Hoxa3, Hoxa10, Hoxd13* and some other regions (8 out 21) showed significant decreased occupancy similar to sperm of F1 (Fig. 6B).

To reveal whether the decreased level of H3K4me3 in F1 is due to the reduction in histone-containing fraction of sperm, we performed ChIP-qPCR using unmodified histone H3 antibody. We found that H3 showed no significant changes at the promoters we analyzed (Fig. S13). Moreover, the sperm protein H3 histone level is similar in control and CD-exposed group (Fig. 6C-D).

This data suggests that the histone-containing fraction is not altered at analyzed genes but rather has decreased H3K4me3 content at analyzed genes in both F1 and F3.

Our results suggest that the alterations in H3K4me3 occupancy in the vicinity of important developmental genes were induced in the prostate of F1 males as well as in sperm of F1 and F3.

4. Discussion

Epidemiological studies have shown that postnatal CD exposure (ie. in men born before 1973, the year in which this insecticide was introduced the French West Indies) is associated with an increased risk of PCa in the French West Indies population (Brureau et al., 2019; Multigner et al., 2010). Whether the generations that are born after 1973, who are *in utero* exposed to CD, have health issues remains an open and unresolved question. Our recent study on CD exposure to pregnant mice showed epigenetic alterations in testis and reproductive defects that were transmitted up to three generations (Gely-Pernot et al., 2018). Therefore, we hypothesized the likelihood of prostate alterations following developmental CD exposure as well as its transgenerational inheritance mediated via epigenetic features. Our data show that developmental exposure to CD increases the occurrence of PIN in both F1 and F3 generations and provides evidence for the involvement of epigenetic histone modifications in the transmission of these effects.

We observed a significant increase in the incidence of PIN phenotype in the directly exposed F1, and an increase in non-directly (F3) exposed mice which did not cross the significance threshold ($p = 0.054$). The appearance of the PIN phenotype occurs when epithelial cells initiate division and crowd in the lumen of the prostate and are considered as a precursor of PCa. Although there are fundamental differences in mouse and human prostate morphology, anatomy and tumorigenesis, mice remain an indispensable model for studying prostate cancer as well as

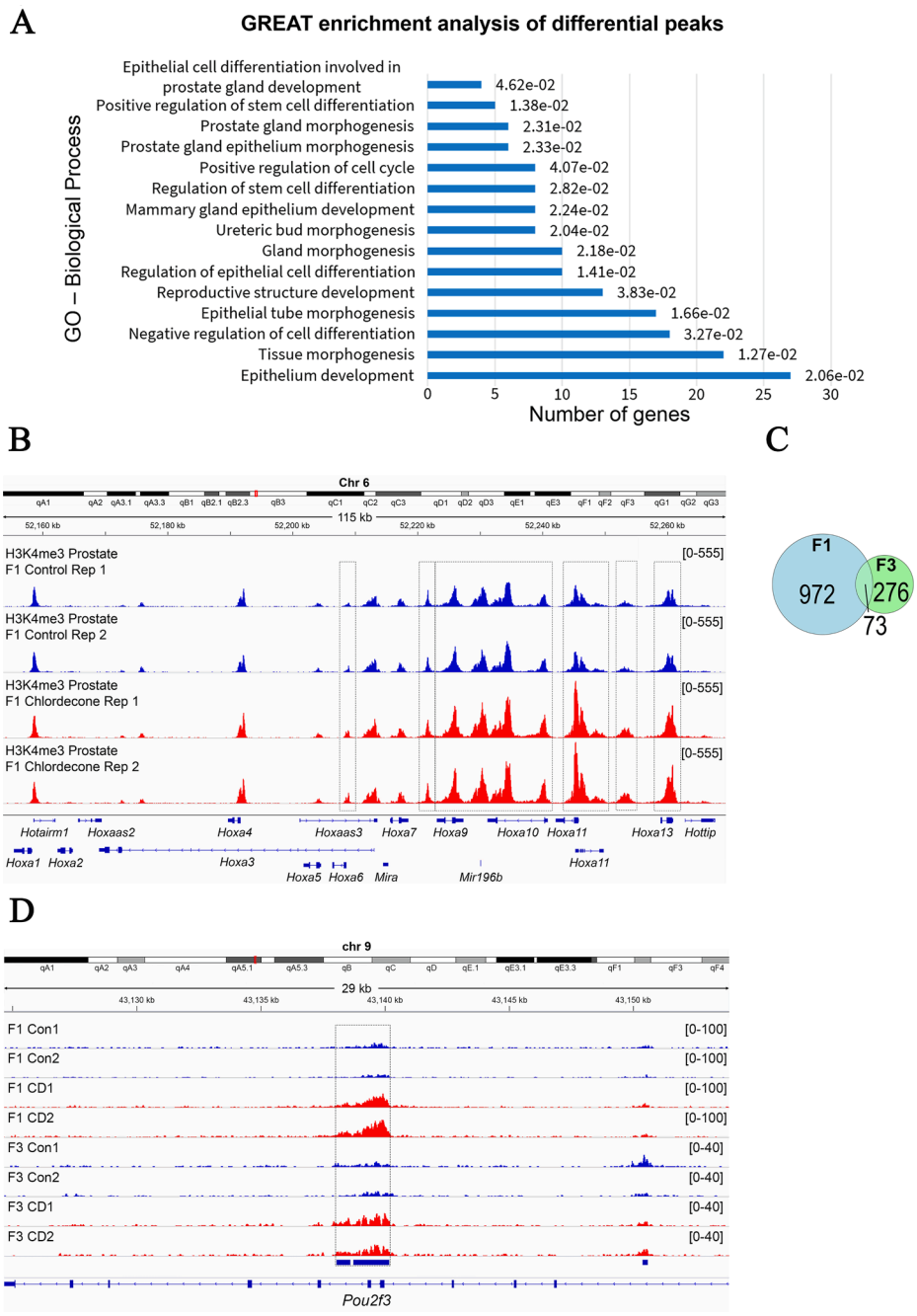

Fig. 5. Gestational exposure of CD leads to the alteration in H3K4me3 occupancy at 129 regions in F1 and at 240 in F3 prostate. (A) Differential peaks were in the vicinity of the genes involved in prostate development. The altered peaks (FC > 2, FDR < 0.05) were assigned to genes and functionally annotated by GREAT. The adjusted p-value is displayed at the end of each bar (binomial test). (B) View from IGV is displaying the increase in mapped reads in CD-derived prostate in the 115 kb-long region including 16 genes from the *Hoxa* family. Peaks from control mice are shown in blue, and from CD-exposed mice are shown in red. Regions with significantly different occupancy are marked with dashed boxes. (C) Venn diagram showing the common genes which have differential peaks in F1 and F3 generations. (D) Differential peaks detected in *Pou2f3* in F1 and F3 prostate ChIP-seq. Regions with significantly different occupancy are marked with dashed boxes. (For interpretation of the references to colour in this figure legend, the reader is referred to the web version of this article.)

transgenerational epigenetic inheritance. Despite the claims that mouse dorsolateral prostate is similar to human prostate (Berquin et al., 2005), the Bar Harbor Histology Panel has clearly stated that no conclusive evidence exists to affirm that any of the mouse prostate lobes are identical to human prostate (Irshad and Abate-Shen, 2013; Shappell et al., 2004). However, histologically, both mouse and human prostate epithelial cells can be differentiated into basal, luminal and neuroendocrine cells. Taking into consideration the facts that rodents are less prone to prostate cancer compared to humans (Bosland and Prinsen, 1990; Shappell et al., 2004) and that the anterior prostate lobe in mice have a higher risk to develop PIN phenotype compared to other lobes (Bhatia-Gaur et al., 1999; Ouyang et al., 2005), we opted to analyze the anterior prostate lobe. Herein, the anterior prostate showed a clear PIN phenotype pattern in F1 and F3 mice indicating pathologic transformation.

We explored the RNA expression changes and epigenetic features of the prostate chromatin to explain the increased PIN phenotype that we observed in CD-derived F1 and F3 generations. We found several genes with important roles in prostate function, such as *Hox family*, to be highly over-expressed in F1 and F3 mice. A strong decrease in *Hoxb13* was detected in F1; mutation in *HOXB13* leads to higher risk of prostate cancer (Ewing et al., 2012), suggesting that CD-induced prostate cells proliferation could be mediated via alteration in *Hoxb13*. It has been shown that HOXA7 could increase cell proliferation through up-regulation of epidermal growth factor receptor in granulosa cells (Zhang et al., 2010). *Hox* genes are important regulators of body plan development (Krumlauf, 1994), are spatially and temporally regulated by epigenetic factors (Noordermeer et al., 2011) and play a critical role in cancer development (Bhatlekar et al., 2014). Upregulation of *Hoxa3* is known to be associated with tumor growth and metastasis in pancreatic (Kuo et al., 2019) and colon cancers (X. Zhang et al., 2018), and its downregulation has been observed in lung adenocarcinoma (Gan et al.,

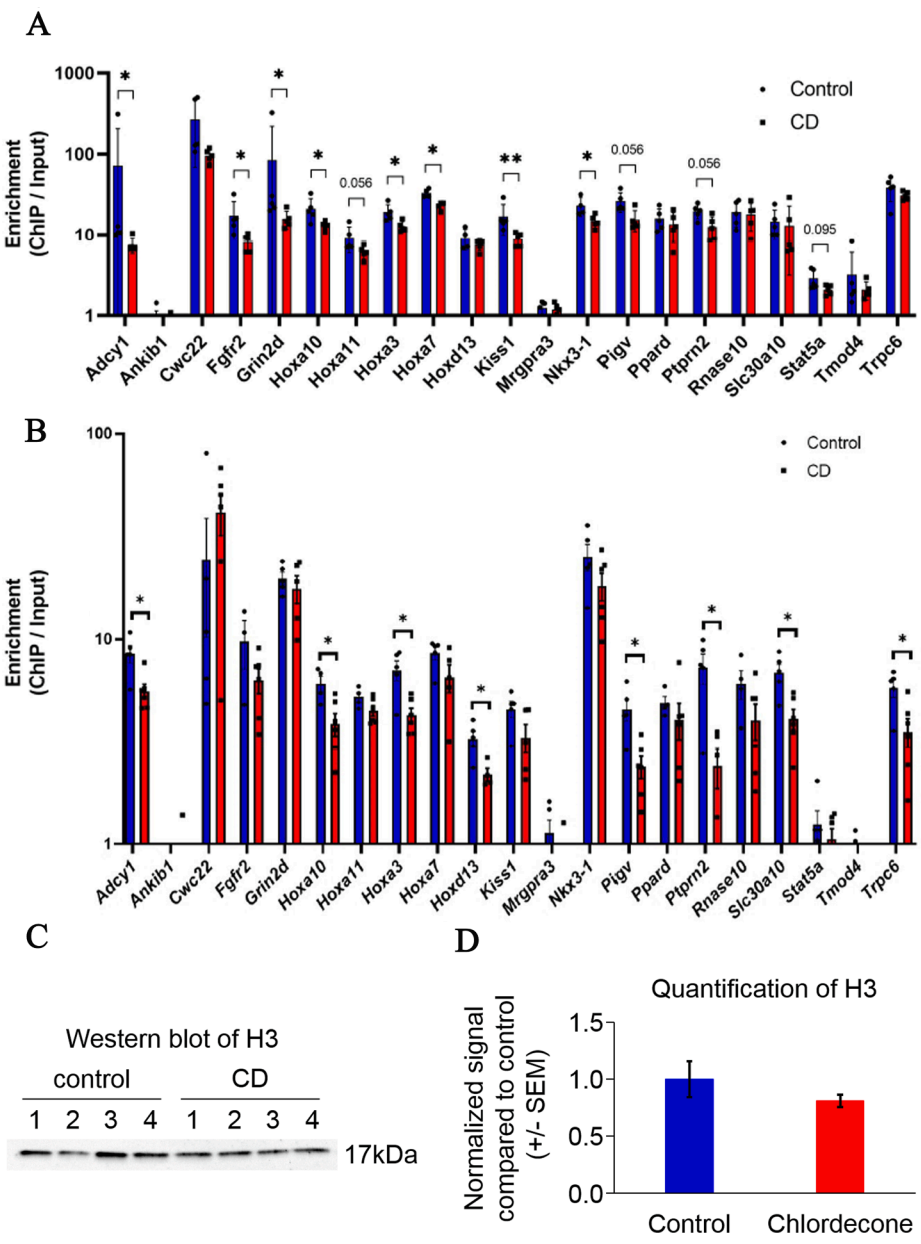

Fig. 6. H3K4me3 occupancy was altered in the vicinity of some genes in the sperm of F1 and F3 mice**, exposed to CD during development.** Histone occupancy of H3K4me3 in F1 (A) and in (B) F3 panel were analyzed by ChIP-qPCR in the sperm. An equal amount of ChIP and input DNA were taken for qPCR. Each value for target genes was normalized to the *Gapdh* region. The data are presented as normalized ChIP to Input ratios compared to control ± SEM. *p < 0.05, **p < 0.01, ***p < 0.001. Promoters with increased occupancy are in red and with decreased occupancy are in blue. (C) Western blot analysis of unmodified H3 in the sperm of F1 mice. Histones were purified from F1 CD-exposed and control sperm were analyzed by Western blot. (D) Quantitative analysis of unmodified H3 protein levels from Western blots was performed using ImageJ software and the data are presented as the normalized signal compared to control ± SEM. (For interpretation of the references to colour in this figure legend, the reader is referred to the web version of this article.)

2018), while *Hoxa7* is implicated in epithelial ovarian (Ota et al., 2007) and liver cancers (Li et al., 2015). Based on our study and given the critical role of *Hoxa* in cancers, we propose that the deregulation of the *Hoxa* cluster could play a role in the development of the PIN phenotype in CD-derived mice.

We also found that gestational exposure to CD causes a dramatic increase in genes associated with hormonal biosynthesis in F1 and F3. Several human prostate studies have reported the upregulation of genes encoding for the key steroidogenic enzymes such as *AKR1C3, CYP17A1, SRD5A1,2,* reviewed in (Armandari et al., 2014). High expression of *AKR1C3, SRD5A1* were found in circulating tumor cells derived from primary prostate cancer, suggesting that steroidogenesis elevation plays an important role in prostate cancer (Mitsiades et al., 2012). In clinical castration-resistant prostate cancer (CRPC) samples, the expression of *AKR1C3* and *17βHSD3* were increased (Pfeiffer et al., 2011), and the overexpression of AKR1C3 were also shown in metastatic CRPC (Montgomery et al., 2008).

The elevated expression of steroidogenesis genes was accompanied with an increased expression of *Esr2* (ERβ) in F1 and F3 progeny, and *Essrg* in F1 males in our study. ESR2 was found to be up-regulated in triple-negative breast cancer cell lines and treatment with ESR2 agonist led to a significant increase in cell proliferation and migration (Austin et al., 2018). Similarly, it is suggested that cancer progression in primary and metastatic adenocarcinoma is mediated via ESR2 signaling (Fixemer et al., 2003). We also detected a large number of genes that are related to extracellular matrix function to be deregulated in F1 and F3. Studies have shown that coordinated actions of estrogens and the 3D network of macromolecules that form the extracellular matrix play an important role in remodeling the matrix for the progression of several types of cancers including prostate cancer, reviewed in (Piperigkou and Karamanos, 2020). Multiple epidemiological studies showed the link between elevated estrogen levels during pregnancy and increased prostate cancer in males (Barker et al., 2012; Henderson et al., 1991). Similar to CD, early life exposure to low-dose BPA increases the incidence of hormone-associated prostate carcinogenesis in animal model as well (Prins et al., 2014) which could be due to the estrogenic properties of both the compounds. In experiments involving humanized mice, exposure to BPA has been shown to increase PIN and the expression of self-

renewal related genes (Prins et al., 2014). It is considered that self-renewal genes are crucial for stem cells maintenance which, in turn, helps in the regeneration of prostate architecture following androgen ablation and are also responsible for replenishing cells during PCa development (Moltzahn and Thalmann, 2013).

Alternatively, we studied liver, an organ where CD primarily accumulates (Egle et al., 1978). We found that the changes induced by CD in liver are dramatic only in F1 generation and not in F3, suggesting that epigenetic memory does not preserve the alterations in the liver or perhaps to a less extent than in reproductive organs. Studies have shown that certain regions in the germline avoid reprogramming (Hill et al., 2018) and preserve the information related to gametogenesis as well as development while the information pertaining to somatic cells are not preserved. *Hox* genes are important for body plan and development; accordingly, the *Hox* gene alterations are possibly preserved in the sperm and affect the developmental program of somatic organs, such as prostate.

4.1. Epigenetic alterations in histone acetylation and methylation marks in CD-exposed prostate

Epigenetics plays a vital role in PCa development (Baumgart and Haendler, 2017) as well as in its transgenerational inheritance (Klukovich et al., 2019). In CD-exposed F1 mice, we observed a global decrease in the histone acetylation levels in the exposed prostate. Because histone H4ac controls DNA accessibility to repair factors, it is conceivable that decreased acetylation could compromise the DNA repair. This is an important observation considering CD's ability to cause DNA damage by increasing 8-oxo-G levels (Legoff et al., 2019a); so, the accessibility to DNA for repair is critical. The described effects on H4ac however, were not transgenerational, at a global level. We did not observe a decrease in H4ac in F3 generation both by IFA and WB methods.

We found that H3K4me3 levels were increased in CD-exposed mice, with some regions being altered in both generations and sperm. The increased H3K4me3 is associated with decreased H3K27me3 levels which is consistent with previous work that found specific counter-balanced levels of these marks in normal and cancerous prostate cells (Ke et al., 2009). The authors reported that these marks act as epigenetic switches; for example, loss of H3K27me3 coupled with a gain of H3K4me3 was associated with high activation of several deregulated genes (Ke et al., 2009), indicating that changes in the ratio of these methylation marks play a role in prostate carcinogenesis. We also observed an increased expression of a major histone lysine methyl transferases (KMTs), *Kmt2d,* in both F1 and F3 PIN-containing prostates compared to control. The protein encoded by *Kmt2d* is a transcriptional regulator of the estrogen receptor genes (Toska et al., 2017) and an overexpression of KMT2D was observed in gastric cancer samples (Xiong et al., 2018), suggesting that *KMT2D* has oncogenic properties. Moreover, most of the differentially expressed genes that we identified in our F3 prostate RNA-seq data has been shown to be preferentially expressed in luminal cells (D. Zhang et al., 2016). In agreement, our immunofluorescence data show that signals for histone marks are higher in luminal cells. From this, it is conceivable that the driver of epigenetic changes arises originally in luminal cells. Moreover, the studies that aimed at elucidating the origin of prostate cancer cells were recently reviewed (D. Zhang et al., 2018); and, while earlier work pointed at basal cells as a point of origin for transformation, more recent studies suggest the luminal origin of transformation of these cells (D. Zhang et al., 2018).

We found a deregulation in the expression levels of *Hox* genes. For these genes, strong relationship between gene expression and histone marks was detected in F1. The increased histone occupancy in *Hoxa13,* which plays a role in embryonic genitourinary (Du and Taylor, 2004; Goodman, 2002) and prostate development (Huang et al., 2007), is associated with unfavorable survival of PCa patients (Dong et al., 2017), which makes this gene one of the strong candidates for "driving" transcriptional activity network change.

Furthermore, we found strong increase in *Pou2f3* and *Tfap2c* H3K4me3 occupancy in F1 and F3, genes, which are normally expressed in keratinocytes. The decrease in *POU2F3* expression was found in cervical cancer (Zhang et al., 2006). The upregulation of *POU2F3* was detected in human colorectal cancer (Goto et al., 2019) and in small cell lung cancer which is a tumor of pulmonary neuroendocrine cells (Huang et al., 2018). These data suggest that like other cancers the neuroendocrine cells in prostate could be responsible for PIN transformation.

We believe that epigenetic change results in a more accessible chromatin structure that could impose favorable conditions for gene over-expression and proliferation activity in CD-exposed mice.

4.2. Transgenerational inheritance of histone H3K4 methylation modifications via sperm

Since changes in histone H3K4me3 occupancy found in the prostate of F1 animals were also detected in the spermatozoa of F1 mice, it is possible that CD-induced changes are inheritable at least at some regions of the genome.

Targeted analyses of histone H3K4me3 mark distribution in the F3 prostate showed that several epigenetic changes were preserved between F1 and F3 generations, including the *Hoxa* cluster. Unlike the bulk of sperm DNA that undergo histone-to-protamine transition, *Hox* family genes preserve their associated histones based on early studies by Hammoud and colleagues (Hammoud et al., 2009) that has been recently confirmed (B. Zhang et al., 2016). Notably, histone occupancy in prostate and sperm had an opposite direction of changes. After fertilization, numerous events contribute to zygote formation and to organ development, and we believe that the complexity of this process could explain the opposite changes in histone H3K4me3 occupancy in prostate and sperm. Hox genes have tissue-specific expression features, and are regulated by higher order chromatin organization, long non-coding RNAs and transcription factor complexes in adult tissues (Yamamoto et al., 2003). We propose that these 'other regulatory factors' might have played a role in the observed results in adult prostate. Further experiments in the embryo are required to reveal the histones fates during early development. Since the changes we observed affect the same regions in F1 sperm and the F3 prostate, we believe that these regions are transgenerationally inherited. A schematic diagram representing the potential pathways that could lead to development of PIN phenotype in prostate of F1 and F3 generations via sperm is provided in Fig. S14.

4.3. Limitations of the study

One of the limitations of this work is that the consequences of epigenetic alterations observed in animal model are not yet confirmed in humans, especially the capacity of CD to promote the tumorigenesis. It is not clear how exactly alterations in *Hoxa* genes lead to prostate PIN in humans. The role of other epigenetic factors such as noncoding RNA has not been determined. We noted that some of the noncoding RNAs are differentially expressed in exposed mice, and the role of these ncRNA in *Hoxa* expression should be addressed in future studies. It is not clear how long the transgenerational effects promoted by CD could last. Since we detected alterations that are still persistent in F3 males, it is possible that 4th or 5th generations still manifest the promoted effects. Thus, further work is required to address those questions and to investigate the human health consequences due to CD contamination.

5. Conclusions

In conclusion, our study provides evidence that developmental exposure to CD results in epigenetic effects on prostate tissue in mice which could be inherited via sperm although common changes observed in F1 and F3 are limited suggesting the role of other factors as well in transmitting the effects. The study has important public health

implications in populations where humans are still exposed to this compound.

CRediT authorship contribution statement

Louis Legoff: Software, Validation, Formal analysis, Investigation, Writing - original draft, Visualization. **Shereen Cynthia D'Cruz:** Investigation, Writing - original draft. **Morgane Lebosq:** Investigation. **Aurore Gely-Pernot:** Investigation. **Katia Bouchekhchoukha:** Investigation. **Christine Monfort:** Formal analysis. **Pierre-Yves Kernanec:** Investigation. **Sergei Tevosian:** Writing - review & editing. **Luc Multigner:** Writing - review & editing. **Fatima Smagulova:** Conceptualization, Supervision, Methodology, Investigation, Writing - original draft.

Declaration of Competing Interest

The authors declare that they have no known competing financial interests or personal relationships that could have appeared to influence the work reported in this paper.

Acknowledgments

The authors are thankful to the H2P2 platform of Rennes for assistance with tissue preparation for histology, and to Pr. Nathalie Rioux-Leclercq for phenotype interpretation. Sequencing was performed by the GenomEast platform, a member of the "France Génomique" consortium (ANR-10-INBS-0009). We acknowledge the GenOuest bioinformatics core facility (https://www.genouest.org) for providing the computing infrastructure.

All sequencing data from this study are publicly available and have been deposited in the National Centre for Biotechnology Information Gene Expression Omnibus (GEO). The accession number is GSE135201.

Funding

This work was supported by Atip-Avenir program (R13139NS) to FS. LL was supported by ARED/INSERM fellowship. This work was also supported by the French National Health Directorate (Grant R20153NN), however, the funder had no role in study design, data collection and analysis, decision to publish, or preparation of the manuscript.

Appendix A. Supplementary material

Supplementary data to this article can be found online at https://doi.org/10.1016/j.envint.2021.106472.

References

Agency for Toxic Substances and Disease Registry (ATSDR), 2019. Toxicological profile for Mirex and Chlordecone (Draft for Public Comment). Atlanta, GA: U.S. Department of Health and Human Services, Public Health Service. Available at: https://www.atsdr.cdc.gov/ToxProfiles/tp66.pdf.

Armandari, I., Hamid, A.R., Verhaegh, G., Schalken, J., 2014. Intratumoral steroidogenesis in castration-resistant prostate cancer: a target for therapy. Prostate Int. 2, 105–113. https://doi.org/10.12954/PI.14063.

Austin, D., Hamilton, N., Elshimali, Y., Pietras, R., Wu, Y., Vadgama, J., 2018. Estrogen receptor-beta is a potential target for triple negative breast cancer treatment. Oncotarget 9, 33912–33930. https://doi.org/10.18632/oncotarget.26089.

Barker, D.J.P., Osmond, C., Thornburg, K.L., Kajantie, E., Eriksson, J.G., 2012. A possible link between the pubertal growth of girls and prostate cancer in their sons. Am. J. Hum. Biol. Off. J. Hum. Biol. Counc. 24, 406–410. https://doi.org/10.1002/ajhb.22222.

Baumgart, S.J., Haendler, B., 2017. Exploiting Epigenetic Alterations in Prostate Cancer. Int. J. Mol. Sci. 18 https://doi.org/10.3390/ijms18051017.

Ben Maamar, M., Nilsson, E., Sadler-Riggleman, I., Beck, D., McCarrey, J.R., Skinner, M. K., 2019. Developmental origins of transgenerational sperm DNA methylation epimutations following ancestral DDT exposure. Dev. Biol. 445, 280–293. https://doi.org/10.1016/j.ydbio.2018.11.016.

Berquin, I.M., Min, Y., Wu, R., Wu, H., Chen, Y.Q., 2005. Expression signature of the mouse prostate. J. Biol. Chem. 280, 36442–36451. https://doi.org/10.1074/jbc.M504945200.

Bhatia-Gaur, R., Donjacour, A.A., Sciavolino, P.J., Kim, M., Desai, N., Young, P., Norton, C.R., Gridley, T., Cardiff, R.D., Cunha, G.R., Abate-Shen, C., Shen, M.M., 1999. Roles for Nkx3.1 in prostate development and cancer. Genes Dev. 13, 966–977. https://doi.org/10.1101/gad.13.8.966.

Bhatlekar, S., Fields, J.Z., Boman, B.M., 2014. HOX genes and their role in the development of human cancers. J. Mol. Med. 92, 811–823. https://doi.org/10.1007/s00109-014-1181-y.

Bosland, M.C., Prinsen, M.K., 1990. Induction of dorsolateral prostate adenocarcinomas and other accessory sex gland lesions in male Wistar rats by a single administration of N-methyl-N-nitrosourea, 7,12-dimethylbenz(a)anthracene, and 3,2'-dimethyl-4-aminobiphenyl after sequential treatment with cyproterone acetate and testosterone propionate. Cancer Res. 50, 691–699.

Boucher, O., Simard, M.-N., Muckle, G., Rouget, F., Kadhel, P., Bataille, H., Chajès, V., Dallaire, R., Monfort, C., Thomé, J.-P., Multigner, L., Cordier, S., 2013. Exposure to an organochlorine pesticide (chlordecone) and development of 18-month-old infants. Neurotoxicology 35, 162–168. https://doi.org/10.1016/j.neuro.2013.01.007.

Brureau, L., Emeville, E., Helissey, C., Thome, J.P., Multigner, L., Blanchet, P., 2019. Endocrine disrupting-chemicals and biochemical recurrence of prostate cancer after prostatectomy: A cohort study in Guadeloupe (French West Indies). Int. J. Cancer. https://doi.org/10.1002/ijc.32287.

Brykczynska, U., Hisano, M., Erkek, S., Ramos, L., Oakeley, E.J., Roloff, T.C., Beisel, C., Schübeler, D., Stadler, M.B., Peters, A.H.F.M., 2010. Repressive and active histone methylation mark distinct promoters in human and mouse spermatozoa. Nat. Struct. Mol. Biol. 17, 679–687. https://doi.org/10.1038/nsmb.1821.

Burton, A., Torres-Padilla, M.-E., 2010. Epigenetic reprogramming and development: a unique heterochromatin organization in the preimplantation mouse embryo. Brief. Funct. Genomics 9, 444–454. https://doi.org/10.1093/bfgp/elq027.

Cabidoche, Y.M., Achard, R., Cattan, P., Clermont-Dauphin, C., Massat, F., Sansoulet, J., 2009. Long-term pollution by chlordecone of tropical volcanic soils in the French West Indies: a simple leaching model accounts for current residue. Environ. Pollut. 157, 1697–1705. https://doi.org/10.1016/j.envpol.2008.12.015.

Chen, Z., Wang, L., Wang, Q., Li, W., 2010. Histone modifications and chromatin organization in prostate cancer. Epigenomics 2, 551–560. https://doi.org/10.2217/epi.10.31.

Conteduca, V., Oromendia, C., Eng, K.W., Bareja, R., Sigouros, M., Molina, A., Faltas, B. M., Sboner, A., Mosquera, J.M., Elemento, O., Nanus, D.M., Tagawa, S.T., Ballman, K.V., Beltran, H., 2019. Clinical features of neuroendocrine prostate cancer. Eur. J. Cancer Oxf. Engl. 1990 (121), 7–18. https://doi.org/10.1016/j.ejca.2019.08.011.

Costet, N., Pelé, F., Comets, E., Rouget, F., Monfort, C., Bodeau-Livinec, F., Linganiza, E. M., Bataille, H., Kadhel, P., Multigner, L., Cordier, S., 2015. Perinatal exposure to chlordecone and infant growth. Environ. Res. 142, 123–134. https://doi.org/10.1016/j.envres.2015.06.023.

Dahl, J.A., Jung, I., Aanes, H., Greggains, G.D., Manaf, A., Lerdrup, M., Li, G., Kuan, S., Li, B., Lee, A.Y., Preissl, S., Jermstad, I., Haugen, M.H., Suganthan, R., Bjørås, M., Hansen, K., Dalen, K.T., Fedorcsak, P., Ren, B., Klungland, A., 2016. Broad histone H3K4me3 domains in mouse oocytes modulate maternal-to-zygotic transition. Nature 537, 548–552. https://doi.org/10.1038/nature19360.

Dong, Y., Cai, Y., Liu, B., Jiao, X., Li, Z.-T., Guo, D.-Y., Li, X.-W., Wang, Y.-J., Yang, D.-K., 2017. HOXA13 is associated with unfavorable survival and acts as a novel oncogene in prostate carcinoma. Future Oncol. Lond. Engl. 13, 1505–1516. https://doi.org/10.2217/fon-2016-0522.

Du, H., Taylor, H.S., 2004. Molecular regulation of mullerian development by Hox genes. Ann. N. Y. Acad. Sci. 1034, 152–165. https://doi.org/10.1196/annals.1335.018.

Egle, J.L., Fernandez, J.B., Guzelian, P.S., Borzelleca, J.F., 1978. Distribution and excretion of chlordecone (Kepone) in the rat. Drug Metab. Dispos. Biol. Fate Chem. 6, 91–95.

Eroschenko, V.P., 1981. Estrogenic activity of the insecticide chlordecone in the reproductive tract of birds and mammals. J. Toxicol. Environ. Health 8, 731–742. https://doi.org/10.1080/15287398109530109.

Ewing, C.M., Ray, A.M., Lange, E.M., Zuhlke, K.A., Robbins, C.M., Tembe, W.D., Wiley, K.E., Isaacs, S.D., Johng, D., Wang, Y., Bizon, C., Yan, G., Gielzak, M., Partin, A.W., Shanmugam, V., Izatt, T., Sinari, S., Craig, D.W., Zheng, S.L., Walsh, P. C., Montie, J.E., Xu, J., Carpten, J.D., Isaacs, W.B., Cooney, K.A., 2012. Germline mutations in HOXB13 and prostate-cancer risk. N. Engl. J. Med. 366, 141–149. https://doi.org/10.1056/NEJMoa1110000.

Fixemer, T., Remberger, K., Bonkhoff, H., 2003. Differential expression of the estrogen receptor beta (ERbeta) in human prostate tissue, premalignant changes, and in primary, metastatic, and recurrent prostatic adenocarcinoma. Prostate 54, 79–87. https://doi.org/10.1002/pros.10171.

Fraga, M.F., Ballestar, E., Villar-Garea, A., Boix-Chornet, M., Espada, J., Schotta, G., Bonaldi, T., Haydon, C., Ropero, S., Petrie, K., Iyer, N.G., Pérez-Rosado, A., Calvo, E., Lopez, J.A., Cano, A., Calasanz, M.J., Colomer, D., Piris, M.Á., Ahn, N., Imhof, A., Caldas, C., Jenuwein, T., Esteller, M., 2005. Loss of acetylation at Lys16 and trimethylation at Lys20 of histone H4 is a common hallmark of human cancer. Nat. Genet. 37, 391–400. https://doi.org/10.1038/ng1531.

Gan, B.-L., He, R.-Q., Zhang, Y., Wei, D.-M., Hu, X.-H., Chen, G., 2018. Downregulation of HOXA3 in lung adenocarcinoma and its relevant molecular mechanism analysed by RT-qPCR, TCGA and in silico analysis. Int. J. Oncol. 53, 1557–1579. https://doi.org/10.3892/ijo.2018.4508.

Gely-Pernot, A., Hao, C., Becker, E., Stuparevic, I., Kervarrec, C., Chalmel, F., Primig, M., Jégou, B., Smagulova, F., 2015. The epigenetic processes of meiosis in male mice are

broadly affected by the widely used herbicide atrazine. BMC Genomics 16. https://doi.org/10.1186/s12864-015-2095-y.
Gely-Pernot, A., Hao, C., Legoff, L., Multigner, L., D'Cruz, S.C., Kervarrec, C., Jégou, B., Tevosian, S., Smagulova, F., 2018. Gestational exposure to chlordecone promotes transgenerational changes in the murine reproductive system of males. Sci. Rep. 8, 10274. https://doi.org/10.1038/s41598-018-28670-w.
Goodman, F.R., 2002. Limb malformations and the human HOX genes. Am. J. Med. Genet. 112, 256–265. https://doi.org/10.1002/ajmg.10776.
Goto, N., Fukuda, A., Yamaga, Y., Yoshikawa, T., Maruno, T., Maekawa, H., Inamoto, S., Kawada, K., Sakai, Y., Miyoshi, H., Taketo, M.M., Chiba, T., Seno, H., 2019. Lineage tracing and targeting of IL17RB+ tuft cell-like human colorectal cancer stem cells. Proc. Natl. Acad. Sci. USA 116, 12996–13005. https://doi.org/10.1073/pnas.1900251116.
Guldner, L., Multigner, L., Héraud, F., Monfort, C., Pierre Thomé, J., Giusti, A., Kadhel, P., Cordier, S., 2010. Pesticide exposure of pregnant women in Guadeloupe: Ability of a food frequency questionnaire to estimate blood concentration of chlordecone. Environ. Res. 110, 146–151. https://doi.org/10.1016/j.envres.2009.10.015.
Guldner, L., Seurin, S., Héraud, F., Multigner, L., 2011. Exposition de la population antillaise au chlordécone. BEH 3-4-5, 25–28.
Hammond, B., Katzenellenbogen, B.S., Krauthammer, N., Mcconnell, J.M., 1979. Estrogenic activity of the insecticide chlordecone (Kepone) and interaction with uterine estrogen receptors. Proc. Natl. Acad. Sci. USA 76, 6641–6645. https://doi.org/10.1073/pnas.76.12.6641.
Hammoud, S.S., Nix, D.A., Zhang, H., Purwar, J., Carrell, D.T., Cairns, B.R., 2009. Distinctive chromatin in human sperm packages genes for embryo development. Nature 460, 473–478. https://doi.org/10.1038/nature08162.
Hao, C., Gely-Pernot, A., Kervarrec, C., Boudjema, M., Becker, E., Khil, P., Tevosian, S., Jégou, B., Smagulova, F., 2016. Exposure to the widely used herbicide atrazine results in deregulation of global tissue-specific RNA transcription in the third generation and is associated with a global decrease of histone trimethylation in mice. Nucleic Acids Res. 44, 9784–9802. https://doi.org/10.1093/nar/gkw840.
Heindel, J.J., Vandenberg, L.N., 2015. Developmental Origins of Health and Disease: A Paradigm for Understanding Disease Etiology and Prevention. Curr. Opin. Pediatr. 27, 248–253. https://doi.org/10.1097/MOP.0000000000000191.
Henderson, B.E., Ross, R.K., Pike, M.C., 1991. Toward the primary prevention of cancer. Science 254, 1131–1138. https://doi.org/10.1126/science.1957166.
Hill, P.W.S., Leitch, H.G., Requena, C.E., Sun, Z., Amouroux, R., Roman-Trufero, M., Borkowska, M., Terragni, J., Vaisvila, R., Linnett, S., Bagci, H., Dharmalingham, G., Haberle, V., Lenhard, B., Zheng, Y., Pradhan, S., Hajkova, P., 2018. Epigenetic reprogramming enables the transition from primordial germ cell to gonocyte. Nature 555, 392–396. https://doi.org/10.1038/nature25964.
Huang, L., Pu, Y., Hepps, D., Danielpour, D., Prins, G.S., 2007. Posterior Hox Gene Expression and Differential Androgen Regulation in the Developing and Adult Rat Prostate Lobes. Endocrinology 148, 1235–1245. https://doi.org/10.1210/en.2006-1250.
Huang, Y.-H., Klingbeil, O., He, X.-Y., Wu, X.S., Arun, G., Lu, B., Somerville, T.D.D., Milazzo, J.P., Wilkinson, J.E., Demerdash, O.E., Spector, D.L., Egeblad, M., Shi, J., Vakoc, C.R., 2018. POU2F3 is a master regulator of a tuft cell-like variant of small cell lung cancer. Genes Dev. 32, 915–928. https://doi.org/10.1101/gad.314815.118.
Huber, J.J., 1965. Some physiological effects of the insecticide Kepone in the laboratory mouse. Toxicol. Appl. Pharmacol. 7, 516–524. https://doi.org/10.1016/0041-008x(65)90036-0.
Irshad, S., Abate-Shen, C., 2013. Modeling prostate cancer in mice: something old, something new, something premalignant, something metastatic. Cancer Metastasis Rev. 32, 109–122. https://doi.org/10.1007/s10555-012-9409-1.
Ke, X.-S., Qu, Y., Rostad, K., Li, W.-C., Lin, B., Halvorsen, O.J., Haukaas, S.A., Jonassen, I., Petersen, K., Goldfinger, N., Rotter, V., Akslen, L.A., Oyan, A.M., Kalland, K.-H., 2009. Genome-Wide Profiling of Histone H3 Lysine 4 and Lysine 27 Trimethylation Reveals an Epigenetic Signature in Prostate Carcinogenesis. PLoS ONE 4. https://doi.org/10.1371/journal.pone.0004687.
Klukovich, R., Nilsson, E., Sadler-Riggleman, I., Beck, D., Xie, Y., Yan, W., Skinner, M.K., 2019. Environmental Toxicant Induced Epigenetic Transgenerational Inheritance of Prostate Pathology and Stromal-Epithelial Cell Epigenome and Transcriptome Alterations: Ancestral Origins of Prostate Disease. Sci. Rep. 9 https://doi.org/10.1038/s41598-019-38741-1.
Krumlauf, R., 1994. Hox genes in vertebrate development. Cell 78, 191–201. https://doi.org/10.1016/0092-8674(94)90290-9.
Kuo, T.-L., Cheng, K.-H., Chen, L.-T., Hung, W.-C., 2019. Deciphering The Potential Role of Hox Genes in Pancreatic Cancer. Cancers 11. https://doi.org/10.3390/cancers11050734.
Legoff, L., Dali, O., D'Cruz, S.C., Suglia, A., Gely-Pernot, A., Hémery, C., Kernanec, P.-Y., Demmouche, A., Kervarrec, C., Tevosian, S., Multigner, L., Smagulova, F., 2019a. Ovarian dysfunction following prenatal exposure to an insecticide, chlordecone, associates with altered epigenetic features. Epigenetics Chromatin 12, 29. https://doi.org/10.1186/s13072-019-0276-7.
Legoff, L., D'Cruz, S.C., Tevosian, S., Primig, M., Smagulova, F., 2019b. Transgenerational Inheritance of Environmentally Induced Epigenetic Alterations during Mammalian Development. Cells 8. https://doi.org/10.3390/cells8121559.
Lesch, B.J., Dokshin, G.A., Young, R.A., McCarrey, J.R., Page, D.C., 2013. A set of genes critical to development is epigenetically poised in mouse germ cells from fetal stages through completion of meiosis. Proc. Natl. Acad. Sci. USA 110, 16061–16066. https://doi.org/10.1073/pnas.1315204110.
Li, Y., Yang, X.H., Fang, S.J., Qin, C.F., Sun, R.L., Liu, Z.Y., Jiang, B.Y., Wu, X., Li, G., 2015. HOXA7 stimulates human hepatocellular carcinoma proliferation through cyclin E1/CDK2. Oncol. Rep. 33, 990–996. https://doi.org/10.3892/or.2014.3668.
Lismer, A., Siklenka, K., Lafleur, C., Dumeaux, V., Kimmins, S., 2020. Sperm histone H3 lysine 4 trimethylation is altered in a genetic mouse model of transgenerational epigenetic inheritance. Nucleic Acids Res. 48, 11380–11393. https://doi.org/10.1093/nar/gkaa712.
Lu, P., Ding, Q., Ding, S., Fan, Y., Li, X., Tian, D., Liu, M., 2017. Transmembrane channel-like protein 8 as a potential biomarker for poor prognosis of hepatocellular carcinoma. Mol. Clin. Oncol. 7, 244–248. https://doi.org/10.3892/mco.2017.1285.
Mamun, A.A., O'Callaghan, M.J., Williams, G.M., Najman, J.M., 2012. Maternal Smoking During Pregnancy Predicts Adult Offspring Cardiovascular Risk Factors – Evidence from a Community-Based Large Birth Cohort Study. PLoS ONE 7. https://doi.org/10.1371/journal.pone.0041106.
McLean, C.Y., Bristor, D., Hiller, M., Clarke, S.L., Schaar, B.T., Lowe, C.B., Wenger, A.M., Bejerano, G., 2010. GREAT improves functional interpretation of cis-regulatory regions. Nat. Biotechnol. 28, 495–501. https://doi.org/10.1038/nbt.1630.
Mitsiades, N., Sung, C.C., Schultz, N., Danila, D.C., He, B., Eedunuri, V.K., Fleisher, M., Sander, C., Sawyers, C.L., Scher, H.I., 2012. Distinct patterns of dysregulated expression of enzymes involved in androgen synthesis and metabolism in metastatic prostate cancer tumors. Cancer Res. 72, 6142–6152. https://doi.org/10.1158/0008-5472.CAN-12-1335.
Moltzahn, F., Thalmann, G.N., 2013. Cancer stem cells in prostate cancer. Transl. Androl. Urol. 2, 242–253. https://doi.org/10.3978/j.issn.2223-4683.2013.09.06.
Montgomery, R.B., Mostaghel, E.A., Vessella, R., Hess, D.L., Kalhorn, T.F., Higano, C.S., True, L.D., Nelson, P.S., 2008. Maintenance of intratumoral androgens in metastatic prostate cancer: a mechanism for castration-resistant tumor growth. Cancer Res. 68, 4447–4454. https://doi.org/10.1158/0008-5472.CAN-08-0249.
Morgan, H.D., Santos, F., Green, K., Dean, W., Reik, W., 2005. Epigenetic reprogramming in mammals. Hum. Mol. Genet. 14 Spec No 1, R47-58. Doi: 10.1093/hmg/ddi114.
Multigner, L., Kadhel, P., Rouget, F., Blanchet, P., Cordier, S., 2016. Chlordecone exposure and adverse effects in French West Indies populations. Environ. Sci. Pollut. Res. Int. 23, 3–8. https://doi.org/10.1007/s11356-015-4621-5.
Multigner, L., Ndong, J.R., Giusti, A., Romana, M., Delacroix-Maillard, H., Cordier, S., Jégou, B., Thome, J.P., Blanchet, P., 2010. Chlordecone exposure and risk of prostate cancer. J. Clin. Oncol. Off. J. Am. Soc. Clin. Oncol. 28, 3457–3462. https://doi.org/10.1200/JCO.2009.27.2153.
Nathanielsz, P.W., 2006. Animal Models That Elucidate Basic Principles of the Developmental Origins of Adult Diseases. ILAR J. 47, 73–82. https://doi.org/10.1093/ilar.47.1.73.
Niedzwiecki, M., Zhu, H., Corson, L., Grunig, G., Factor, P.H., Chu, S., Jiang, H., Miller, R.L., 2012. Prenatal exposure to allergen, DNA methylation, and allergy in grandoffspring mice. Allergy 67, 904–910. https://doi.org/10.1111/j.1398-9995.2012.02841.x.
Noordermeer, D., Leleu, M., Splinter, E., Rougemont, J., De Laat, W., Duboule, D., 2011. The dynamic architecture of Hox gene clusters. Science 334, 222–225. https://doi.org/10.1126/science.1207194.
Ota, T., Blake Gilks, C., Longacre, T., Leung, P.C.K., Auersperg, N., 2007. HOXA7 in Epithelial Ovarian Cancer: Interrelationships Between Differentiation and Clinical Features. Reprod. Sci. 14, 605–614. https://doi.org/10.1177/1933719107307781.
Ouyang, X., DeWeese, T.L., Nelson, W.G., Abate-Shen, C., 2005. Loss-of-function of Nkx3.1 promotes increased oxidative damage in prostate carcinogenesis. Cancer Res. 65, 6773–6779. https://doi.org/10.1158/0008-5472.CAN-05-1948.
Pfeiffer, M.J., Smit, F.P., Sedelaar, J.P.M., Schalken, J.A., 2011. Steroidogenic enzymes and stem cell markers are upregulated during androgen deprivation in prostate cancer. Mol. Med. Camb. Mass 17, 657–664. https://doi.org/10.2119/molmed.2010.00143.
Phipson, B., Lee, S., Majewski, I.J., Alexander, W.S., Smyth, G.K., 2016. Robust hyperparameter estimation protects against hypervariable genes and improves power to detect differential expression. Ann. Appl. Stat. 10, 946–963. https://doi.org/10.1214/16-AOAS920.
Piperigkou, Z., Karamanos, N.K., 2020. Estrogen receptor-mediated targeting of the extracellular matrix network in cancer. Semin. Cancer Biol. 62, 116–124. https://doi.org/10.1016/j.semcancer.2019.07.006.
Prins, G.S., Hu, W.-Y., Shi, G.-B., Hu, D.-P., Majumdar, S., Li, G., Huang, K., Nelles, J.L., Ho, S.-M., Walker, C.L., Kajdacsy-Balla, A., van Breemen, R.B., 2014. Bisphenol A promotes human prostate stem-progenitor cell self-renewal and increases in vivo carcinogenesis in human prostate epithelium. Endocrinology 155, 805–817. https://doi.org/10.1210/en.2013-1955.
Raudvere, U., Kolberg, L., Kuzmin, I., Arak, T., Adler, P., Peterson, H., Vilo, J., 2019. g: Profiler: a web server for functional enrichment analysis and conversions of gene lists (2019 update). Nucleic Acids Res. 47, W191–W198. https://doi.org/10.1093/nar/gkz369.
Reik, W., Dean, W., Walter, J., 2001. Epigenetic reprogramming in mammalian development. Science 293, 1089–1093. https://doi.org/10.1126/science.1063443.
Samans, B., Yang, Y., Krebs, S., Sarode, G.V., Blum, H., Reichenbach, M., Wolf, E., Steger, K., Dansranjavin, T., Schagdarsurengin, U., 2014. Uniformity of Nucleosome Preservation Pattern in Mammalian Sperm and Its Connection to Repetitive DNA Elements. Dev. Cell 30, 23–35. https://doi.org/10.1016/j.devcel.2014.05.023.
Seisenberger, S., Andrews, S., Krueger, F., Arand, J., Walter, J., Santos, F., Popp, C., Thienpont, B., Dean, W., Reik, W., 2012. The Dynamics of Genome-wide DNA Methylation Reprogramming in Mouse Primordial Germ Cells. Mol. Cell 48, 849–862. https://doi.org/10.1016/j.molcel.2012.11.001.
Shappell, S.B., Thomas, G.V., Roberts, R.L., Herbert, R., Ittmann, M.M., Rubin, M.A., Humphrey, P.A., Sundberg, J.P., Rozengurt, N., Barrios, R., Ward, J.M., Cardiff, R.D., 2004. Prostate pathology of genetically engineered mice: definitions and

classification. The consensus report from the Bar Harbor meeting of the Mouse Models of Human Cancer Consortium Prostate Pathology Committee. Cancer Res. 64, 2270–2305.

Siklenka, K., Erkek, S., Godmann, M., Lambrot, R., McGraw, S., Lafleur, C., Cohen, T., Xia, J., Suderman, M., Hallett, M., Trasler, J., Peters, A.H., Kimmins, S., 2015. Disruption of histone methylation in developing sperm impairs offspring health transgenerationally. Science 350, aab2006. https://doi.org/10.1126/science.aab2006.

Skinner, M.K., Manikkam, M., Guerrero-Bosagna, C., 2010. Epigenetic transgenerational actions of environmental factors in disease etiology. Trends Endocrinol. Metab. TEM 21, 214–222. https://doi.org/10.1016/j.tem.2009.12.007.

Tabet, E., Genet, V., Tiaho, F., Lucas-Clerc, C., Gelu-Simeon, M., Piquet-Pellorce, C., Samson, M., 2016. Chlordecone potentiates hepatic fibrosis in chronic liver injury induced by carbon tetrachloride in mice. Toxicol. Lett. 255, 1–10. https://doi.org/10.1016/j.toxlet.2016.02.005.

Taniguchi, A., Suga, R., Matsumoto, K., 2000. Expression and transcriptional regulation of the human alpha1, 3-fucosyltransferase 4 (FUT4) gene in myeloid and colon adenocarcinoma cell lines. Biochem. Biophys. Res. Commun. 273, 370–376. https://doi.org/10.1006/bbrc.2000.2929.

Toska, E., Osmanbeyoglu, H.U., Castel, P., Chan, C., Hendrickson, R.C., Elkabets, M., Dickler, M.N., Scaltriti, M., Leslie, C.S., Armstrong, S.A., Baselga, J., 2017. PI3K pathway regulates ER-dependent transcription in breast cancer through the epigenetic regulator KMT2D. Science 355, 1324–1330. https://doi.org/10.1126/science.aah6893.

Vallet-Erdtmann, V., Tavernier, G., Contreras, J.A., Mairal, A., Rieu, C., Touzalin, A.-M., Holm, C., Jégou, B., Langin, D., 2004. The testicular form of hormone-sensitive lipase HSLtes confers rescue of male infertility in HSL-deficient mice. J. Biol. Chem. 279, 42875–42880. https://doi.org/10.1074/jbc.M403495200.

Wadhwa, P.D., Buss, C., Entringer, S., Swanson, J.M., 2009. Developmental Origins of Health and Disease: Brief History of the Approach and Current Focus on Epigenetic Mechanisms. Semin. Reprod. Med. 27, 358–368. https://doi.org/10.1055/s-0029-1237424.

Xiong, W., Deng, Zhenxuan, Tang, Y., Deng, Zhenwei, Li, M., 2018. Downregulation of KMT2D suppresses proliferation and induces apoptosis of gastric cancer. Biochem. Biophys. Res. Commun. 504, 129–136. https://doi.org/10.1016/j.bbrc.2018.08.143.

Yamamoto, M., Takai, D., Yamamoto, Fumiya, Yamamoto, Fumiichiro, 2003. Comprehensive expression profiling of highly homologous 39 hox genes in 26 different human adult tissues by the modified systematic multiplex RT-pCR method reveals tissue-specific expression pattern that suggests an important role of chromosomal structure in the regulation of hox gene expression in adult tissues. Gene Expr. 11, 199–210. https://doi.org/10.3727/000000003108749071.

Zhang, B., Zheng, H., Huang, B., Li, W., Xiang, Y., Peng, X., Ming, J., Wu, X., Zhang, Y., Xu, Q., Liu, W., Kou, X., Zhao, Y., He, W., Li, C., Chen, B., Li, Y., Wang, Q., Ma, J., Yin, Q., Kee, K., Meng, A., Gao, S., Xu, F., Na, J., Xie, W., 2016a. Allelic reprogramming of the histone modification H3K4me3 in early mammalian development. Nature 537, 553–557. https://doi.org/10.1038/nature19361.

Zhang, D., Park, D., Zhong, Y., Lu, Y., Rycaj, K., Gong, S., Chen, X., Liu, X., Chao, H.-P., Whitney, P., Calhoun-Davis, T., Takata, Y., Shen, J., Iyer, V.R., Tang, D.G., 2016b. Stem cell and neurogenic gene-expression profiles link prostate basal cells to aggressive prostate cancer. Nat. Commun. 7 https://doi.org/10.1038/ncomms10798.

Zhang, D., Zhao, S., Li, X., Kirk, J.S., Tang, D.G., 2018a. Prostate Luminal Progenitor Cells in Development and Cancer. Trends Cancer 4, 769–783. https://doi.org/10.1016/j.trecan.2018.09.003.

Zhang, X., Liu, G., Ding, L., Jiang, T., Shao, S., Gao, Y., Lu, Y., 2018b. HOXA3 promotes tumor growth of human colon cancer through activating EGFR/Ras/Raf/MEK/ERK signaling pathway. J. Cell. Biochem. 119, 2864–2874. https://doi.org/10.1002/jcb.26461.

Zhang, Y., Huang, Q., Cheng, J.-C., Nishi, Y., Yanase, T., Huang, H.-F., Leung, P.C., 2010. Homeobox A7 increases cell proliferation by up-regulation of epidermal growth factor receptor expression in human granulosa cells. Reprod. Biol. Endocrinol. RBE 8, 61. https://doi.org/10.1186/1477-7827-8-61.

Zhang, Z., Huettner, P.C., Nguyen, L., Bidder, M., Funk, M.C., Li, J., Rader, J.S., 2006. Aberrant promoter methylation and silencing of the POU2F3 gene in cervical cancer. Oncogene 25, 5436–5445. https://doi.org/10.1038/sj.onc.1209530.